JOURNAL OF GEOPHYSICAL RESEARCH, VOL. 104, NO. D14, PAGES 16,673–16,690, JULY 27, 1999

Potential impacts on Colorado Rocky Mountain weather due to land use changes on the adjacent Great Plains

Thomas N. Chase and Roger A. Pielke Sr.

Department of Atmospheric Science and Graduate Degree Program in Ecology
Colorado State University, Fort Collins

Timothy G. F. Kittel[1]

Climate and Global Dynamics Division, National Center for Atmospheric Research, Boulder, Colorado

Jill S. Baron[1] and Thomas J. Stohlgren[1]

Midcontinent Ecological Science Center, Biological Resources Division, U.S. Geological Survey
Fort Collins, Colorado

Abstract. Evidence from both meteorological stations and vegetational successional studies suggests that summer temperatures are decreasing in the mountain–plain system in northeast Colorado, particularly since the early 1980s. These trends are coincident with large changes in regional land cover. Trends in global, Northern Hemisphere and continental surface temperatures over the same period are insignificant. These observations suggest that changes in the climate of this mountain–plain system may be, in some part, a result of localized forcing mechanisms. In this study the effects of land use change on the northern Colorado plains, where large regions of grasslands have been transformed into both dry and irrigated agricultural lands, on regional weather is examined in an effort to understand this local deviation from larger-scale trends. We find with high-resolution numerical simulations of a 3-day summer period using a regional atmospheric–land surface model that replacing grasslands with irrigated and dry farmland can have impacts on regional weather and therefore climate which are not limited to regions of direct forcing. Higher elevations remote from regions of land use change are affected as well. Specifically, cases with altered landcover had cooler, moister boundary layers, and diminished low-level upslope winds over portions of the plains. At higher elevations, temperatures also were lower as was low-level convergence. Precipitation and cloud cover were substantially affected in mountain regions. We advance the hypothesis that observed land use changes may have already had a role in explaining part of the observed climate record in the northern Colorado mountain–plain system.

1. Introduction

While large-scale deforestation, especially in the tropics, has been identified as a potential source of local and global climate impacts [*Zhang et al.*, 1996; *Bonan et al.*, 1992; *Chase et al.*, 1996], the effects on regional weather and climate due to localized changes in land use in the midlatitudes is relatively undocumented (e.g., see *Cotton and Pielke* [1995] for a survey as of 1992). Significant disruptions in the natural state of the land surface at midlatitudes can be seen to perhaps no greater extent than on the Great Plains in northeastern Colorado. In the last century, large portions of the short-grass steppe which once almost exclusively covered the region have been replaced with areas of irrigated and nonirrigated crop and managed grazing lands [*Gutman et al.*, 1997]. While many of these changes were made before midcentury, the process is ongoing. A 50% increase in the number of irrigated acres in this region occurred between 1974 and 1980 (Colorado Department of Agriculture data derived from the Census of Agriculture, U.S. Commerce Department available at http://www.ag.state.co.us/Resource/stat_list.htm.), while recent population growth is generating more urban and semiurban land cover.

The direct effects of land cover change in the plains are dramatic increases in soil moisture in warm seasons due to irrigation, as well as changes in albedo, aerodynamic roughness, and other surface properties. These direct influences on surface characteristics may initiate indirect effects on local weather and climate in two differing ways. First, the large-scale change of averaged properties of a region can affect climate at all scales by altering surface radiation balances and surface flux partitioning over the entire region [e.g., *Garratt*, 1993; *Sud et al.*, 1988].

Second, discontinuities in surface properties within a region can generate mesoscale circulations, both in models and in observations [*Segal et al.*, 1989; *Vidale*, 1998], which would not exist otherwise. These circulations can be similar in magnitude to the typical sea breeze and may interfere constructively or destructively with any other ambient atmospheric circulation [e.g., *Ookouchi et al.*, 1984; *Segal et al.*, 1988, 1989; *Lee*, 1992; *Seth and Giorgi*, 1996; *Mahfouf et al.*, 1987; *Avissar*, 1995].

[1]Also at Natural Resource Ecology Laboratory, Colorado State University, Fort Collins.

Paper number 1999JD900118.
0148-0227/99/1999JD900118$09.00

Table 1. Trend in Average July Temperature and Significance p Value for 62, 30, and 15-year Time Series

	1934–1995		1966–1995		1981–1995	
	Slope	p	Slope	p	Slope	p
Global	0.0039	<0.01	0.0136	<0.01	−0.0125	ns
Northern Hemisphere	0.0028	0.04	0.0146	<0.01	0.0074	ns
U.S.	−0.0093	0.02	−0.0025	ns	−0.0331	ns
SW U.S.	−0.0034	ns	−0.0121	ns	−0.0266	ns
Colorado	−0.0137	0.02	−0.0215	ns	−0.1033	<0.01
NE Colorado*	−0.0092	ns	−0.0324	0.10	−0.1274	<0.01
SE Colorado*	−0.0179	0.03	−0.0360	0.09	−0.1234	<0.01
Western Colorado*	−0.0089	0.08	−0.0267	0.07	−0.0828	0.08

Trend, in °C yr^{-1}, is slope of the linear regression line; ns, nonsignificant trends ($p > 0.1$).
*These regions have unweighted averages from individual station values.

These circulations may also provide a region favored for low-level convergence and convective activity [*Pielke et al.*, 1993].

There is some confirmation of effects on weather due to the presence of agricultural vegetation in the observational record. In northern Texas, *Barnston and Schickedanz* [1984] discovered an increase in precipitation in regions with heavy irrigation. A general cooling of surface temperatures of 1–2°C was also reported in irrigated regions, though the net effect was a slight increase in convective instability (a decrease in lifted index) due to increased moisture. *Beebe* [1974] found irrigation to enhance severe storms in Texas by increasing available energy. In a 2-year observational study of shallow cumulus cloud development in the midwestern United States, *Rabin and Martin* [1996] found that the average characteristics of soil and vegetation cover may exert as strong a forcing on the development of cumulus clouds, as does the sloping terrain which characterizes the region. On the other hand, *Fowler and Helvey* [1974] found little effect from widespread irrigation in Washington State.

We are trying to answer three questions. What has been the effect on weather and, potentially, climate of changing land use on the Great Plains? What interactions between the plains and mountains allow those effects to be transmitted to higher elevations? Finally, if they are transmitted, how do they affect weather and climate in the higher altitudes of the Rocky Mountains? In an attempt to answer these questions we present a regional temperature trend analysis in section 2. We then present results from high-resolution, numerical model simulations of the atmosphere coupled with a land-surface biophysics model. We applied this model in a case study covering the 3 days from July 30 to August 2, 1992. These days were chosen to represent climatological conditions in the region and were characterized by weak synoptic forcing. Cloudiness and precipitation were therefore diurnally forced by the regional circulation rather than by broader-scale synoptic conditions.

2. Comparative Temperature Trends

The possibility that the climate of northeastern Colorado has been affected by changes in land cover due to human activity is suggested by regional temperature trends. Decreasing northeastern Colorado summer temperatures have been reported in the past [*Greenland et al.*, 1995; *Stohlgren et al.*, 1998]. Also decreased solar radiation was reported at some high-elevation sites [*Williams et al.*, 1996]. Recent studies of plant successional trends and watershed discharge in the northeastern Colorado mountains also indicated a middle to high elevation cooling over the last 50–100 years [*Stohlgren et al.*, 1998].

As a comparison, we present the July average temperature regression slopes for area averages over the globe, the Northern Hemisphere, the continental United States, and the southwestern United States region in Table 1 along with unweighted area-averaged trends for 10 northeastern Colorado stations, 5 southeastern Colorado stations, and 14 western Colorado stations for a 62-year time series as well as two shorter periods. The global and hemispheric data are from *Vinnikov et al.* [1994] with more recent data filled in with Goddard Institute for Space Studies surface temperature data [*Hansen and Lebedeff*, 1987; *Reynolds and Smith*, 1994]. The non-Colorado U.S. data were taken from the National Climatic Data Center (NCDC) Web site [*Karl et al.*, 1986]. Regions within the United States are defined by the NCDC and are areally weighted and averaged. Regions within Colorado were defined for the purposes of this paper and represent straight averages. Western Colorado consists of all portions of the state west of the eastern plains. (Refer to topography in Figure 2.) Northeastern Colorado and southeastern Colorado were divided at roughly half the states north-south extent. Specific stations in each region are listed in the appendix.

The 62-year time series has global and northern hemisphere temperatures rising significantly, while the United States and Colorado temperatures declined significantly. Southwestern U.S. temperatures showed no trends. Colorado as a whole had a significant cooling over this period driven by cooling in western and southeastern Colorado.

In the 30-year time series, global and northern hemispheric warming remained significant. Regional time series showed no significant trends, though the three Colorado subregions all had weakly significant ($p = 0.1$–0.05) cooling. The magnitude of the Colorado cooling trend increased from the 62-year trend and was much larger in the eastern half of the state.

Over the 15-year time series, all scales larger than the state of Colorado are trendless. However, Colorado as a whole exhibits a strong, significant cooling which is several times larger than the trend in the 30-year time series. This is also the case with the three Colorado subregions. While southeastern Colorado had the largest trend in the 62- and 30-year time series, northeastern Colorado now has the largest trend. The western

Table 2. Average Spearman Rank Correlation Coefficient r Between 10 Northeastern Colorado Stations and the Averaged Time Series for the Region Listed and Average Significance p Value for Three Time Periods

	1934–1995		1966–1995		1981–1995	
	r	p	r	p	r	p
Global	0.04	*	0.01	*	−0.06	*
North Hemisphere	0.12	*	0.05	*	0.03	*
U.S.	0.65	<0.01	0.63	<0.01	0.45	*
SW U.S.	0.49	<0.01	0.43	<0.01	0.37	*
Colorado	0.77	<0.01	0.80	<0.01	0.72	<0.01
West Colorado	0.61	<0.01	0.51	<0.01	0.49	*
SE Colorado	0.77	<0.01	0.78	<0.01	0.56	0.03
NE Colorado	0.85	<0.01	0.87	<0.01	0.82	<0.01

Region compositions are described in the appendix.
*Average p value is >0.1.

Colorado trend is quite a bit weaker than in the two eastern regions, which seem to have had similar responses over time.

The regression results give little evidence that northeastern Colorado July cooling trends are coupled with the broadest-scale trends. There is some indication, however, that trends in northeastern Colorado and southeastern Colorado are coupled to some degree. In order to examine this further, 62-year, 30-year, and 15-year time series for 10 northeastern Colorado station were correlated using Spearman's rank correlation coefficients with all larger-scale regional averages and with each of the other Colorado stations used in this study. The results of these correlations and significance estimates are presented in Table 2.

There is no significant correlation between northeastern Colorado stations and global and hemispheric trends on any timescale. For the two longest timescales (30 and 62 years), all other regions are significantly, if weakly, correlated with northeastern Colorado. Only Colorado as a whole and southeastern Colorado region have a substantial (defined here as >50% of the variance explained or $r = 0.7$) impact on northeastern Colorado temperatures. Moreover, these correlations dramatically decrease during the last 15 years of the time series so that southeast Colorado temperatures explain 31% of the variance in northeastern Colorado temperatures during this period, while the average Colorado time series explains 52%. The correlation between northeastern Colorado and the average time series of northeastern Colorado stations is consistently strong and remains at or above 0.82 in all three time periods.

Thus it appears that the highly significant decreases in temperatures over the last 15 years in northeastern Colorado are, to some degree, a localized phenomenon and have occurred subsequent to large increases in the area of irrigated agricultural land in northeastern Colorado. We next discuss the dominant summertime circulation pattern in this region which links the weather and climate of mountain and plains and how observed landcover change might affect it.

3. Mountain-Plains Circulation

During intervals of weak synoptic-scale winds, such as generally occur under summer high-pressure systems, a regularly observed feature in northeastern Colorado (and other mountain-plains/mountain-valley systems) is a regional circulation which flows from the plains upslope toward the highest topography during the day and reverses direction at night [*Toth and Johnson*, 1984; *Wolyn and McKee*, 1994]. This mostly east-west circulation is driven by daytime heating on a topographical gradient which warms higher elevations to a greater degree than air at the same altitude over the plains. The opposite chain of events occurs at night. A horizontal pressure gradient is created which drives a circulation which regularly reaches 5–10 m s^{-1} in magnitude. This circulation dominates the summer climatology of northeastern Colorado and is related to summer rainfall because low-level convergence is initiated near the highest topography as the local, low-level easterlies converge with ambient westerlies [*Toth and Johnson*, 1984]. This provides forcing for the initiation of convective rainstorms given favorable environmental conditions. These storms often travel eastward onto the plains under the influence of large-scale westerlies as the day continues.

The generation of circulation C in time by the solenoidal term in the circulation theorem describes the spin up of the mountain-plains circulation. By Stoke's theorem, circulation can be expressed as a surface integral of vorticity, where the surface integral is taken over a x-z plane circuit:

$$\frac{\partial C}{\partial t} = \int\int_s \frac{\partial \eta}{\partial t}\, ds = \int\int_s g\nabla \times \hat{\mathbf{k}}\left(\frac{\alpha'}{\alpha_0^2}\right)$$

$$\approx \int\int_s g\nabla \times \hat{\mathbf{k}}\left(\frac{\theta'}{\alpha_0\theta_0}\right) \qquad (1)$$

where η represents the vertical component of the total vorticity vector, g is the gravitational acceleration, α_0 is the area-averaged specific volume, α' is the specific volume perturbation, θ_0 is the area-averaged potential temperature, θ' is perturbation potential temperature, and $\hat{\mathbf{k}}$ is a vertical coordinate unit vector.

The approximate integral on the right-hand side of (1) is suitable for shallow systems [*Pielke and Segal*, 1986] and indicates that the strength of this circulation is a direct result of the magnitude of the horizontal temperature gradient and the depth to which this gradient exists. *Atkinson* [1981] points out that temperature differences of only fractions of a degree are effective in spinning up circulations such as this and cites *Wenger*'s [1923] rough calculation that near-slope horizontal velocity U is $\sim 9\Delta T$ m s^{-1}, where T is the temperature in degrees Celsius. Therefore a quite small change in temperature, 0.1°, for example, will change the magnitude of the cir-

culation by ~1 m s^{-1}. This is ~10–20% of the average magnitude of observed northern Colorado circulations [*Toth and Johnson*, 1984; *Wolyn and McKee*, 1994].

The simplest order of magnitude calculation of the sensitivity of the initiation of convective activity to changes in surface conditions can be performed using conservation of mass arguments. We assume a two-dimensional slice through the domain from east to west and assume a vertical barrier 10 km high occurs on the western boundary. This barrier represents the Continental Divide. Assuming an incompressible atmosphere, the two-dimensional continuity equation is written

$$\frac{\partial U}{\partial X} + \frac{\partial W}{\partial Z} = 0, \tag{2}$$

where U and W are the horizontal and vertical velocity components, respectively, and X and Z are the horizontal and vertical coordinates. We assume negligible large-scale winds in the lower atmosphere and integrate over the east-west extent of the mountain-plains circulation from the Continental Divide out to where the circulation is no longer felt (i.e., where U = 0; of the order of 100 km). Vertical velocities are defined to be zero over the domain except within a 20-km region just east of the barrier (representing the leeside region of low-level convergence). By integrating vertically over the depth of the circulation (assumed to be the depth of the boundary layer) and assuming no vertical motion at the bottom boundary we arrive at an expression for the change in vertical velocity in the convergent zone due to changes in horizontal winds across the domain. Applying this equation to two cases, a control and a perturbed case (designated by subscripts 1 and 2), we find that the change in vertical velocity in the leeside convergent zone between the two cases can be expressed as

$$W_2 - W_1 = \frac{(\Delta U_1 - \Delta U_2)(\Delta Z)}{(\Delta X)}. \tag{3}$$

Therefore a change in vertical velocity at the top of the boundary layer is driven by a difference in the gradient of easterlies across the domain. Applying the realistic numbers $\Delta U_1 - \Delta U_2$ = 0.2 m s^{-1}, ΔX = 20,000 m, and ΔZ = 1000 m, we obtain a change in vertical velocity at the top of the boundary layer in the convergent zone of 1 cm s^{-1}. We can relate the above calculation to the minimum vertical velocity at the top of the boundary layer necessary to initiate convection (W_{MIN}) by [e.g., *Bluestein*, 1992]

$$W_{MIN} = \sqrt{2CIN}, \tag{4}$$

where CIN is the convective inhibition (in J kg^{-1}) which is defined as the vertically integrated negative buoyancy a parcel must overcome by heating or mechanical means in order to freely convect. Equation (4) indicates that the strength of CIN that the rising air must overcome increases as a function of the vertical velocity (W) squared. Therefore small changes in vertical motion can have significant effects on the ability to initiate convection. For example, a 5% increase in W from 10.0 to 10.5 cm s^{-1} increases the amount of negative buoyancy that a parcel can overcome by 10% and thereby enhances the potential for convective activity. These highly simplified calculations suggest that the generation of convective activity near the Continental Divide is quite sensitive to the magnitude of the mountain-plains circulation which, in turn, is very sensitive to changes in east-west temperature gradient created by changes in surface conditions.

The potential effects of changes in low-level atmospheric moisture and temperature on the strength of convection or on the atmosphere's ability to maintain convection once it is initiated must also be considered. These effects are measured by the convective available potential energy (CAPE) of the atmosphere which is defined as the vertically integrated positive buoyancy. CAPE is highly sensitive to changes both in low-level moisture and heat [e.g., *Bluestein*, 1992], and changes in its distribution are expected to strongly affect convective activity.

On the basis of the above analysis we demonstrate that the mountain-plains circulation is a mechanism whereby the weather and climate of mountains and plains interact. We hypothesize that observed changes in land use on the plains are extensive enough to have altered the mean summertime mountain-plains circulation thereby affecting climate at higher elevations some distance from the plains. These effects potentially exist in the magnitude and westward penetration of the low-level easterlies generated during the day and in the strength of low-level convergence, cloud cover, and precipitation near the Continental Divide. It may also affect the amount of moisture and heat transported to higher elevations during the day by the low-level regional circulation and so affect CAPE values. This is one mechanism by which changes in plains surface properties might be communicated to remote regions and is a mechanism which can be investigated using a numerical model.

4. Experiment and Model Description

We used the Colorado State University Regional Atmospheric Modeling System (RAMS) Version 3b [*Pielke et al.*, 1992] to perform integrations. RAMS is a comprehensive regional-scale numerical model of the atmosphere that includes land surface and subsurface physical processes. The radiation parameterization includes the effects of the important atmospheric gases but has no interaction with condensed water species [*Mahrer and Pielke*, 1977]. A turbulence closure parameterization following *Smagorinsky*'s [1963] deformation K coefficients is used. Land-surface/atmosphere interaction is based on a bulk aerodynamic formulation of vertical fluxes of heat, momentum, and moisture from the surface [*Louis*, 1979]. An eight-level soil model stretched to a total depth of 1 m has been used to explicitly calculate the moisture and heat content of each subsurface layer [*Tremback and Kessler*, 1985]. Vegetation covers a specified fraction of each grid cell and is described by a single level. Vegetation properties (e.g., albedo, vegetated fraction, and roughness length) are all functions of surface vegetation category, and values are those used in the Biosphere Atmosphere Transfer Scheme [*Dickinson et al.*, 1993] (e.g., Table 1). A constant leaf area of 1.0 was used for all vegetation types. Surface types in this region are short grassland, evergreen forest, mixed woodland, alpine tundra, dry agriculture, and irrigated agriculture.

The atmospheric portion of the model has 24 vertical layers reaching ~20 km into the atmosphere. The first vertical level is at 48 m, with subsequent levels beginning at 110-m intervals and stretching to a maximum of 1500 m near the top of the model volume. This configuration allows adequate resolution of near-surface features while avoiding prohibitive computational expense simulating the upper atmosphere. In the horizontal, we used two interacting, nested grids with grid cell spacings of 24 km and 6.5 km, respectively (Figure 1). The coarse grid covers much of the western United States and

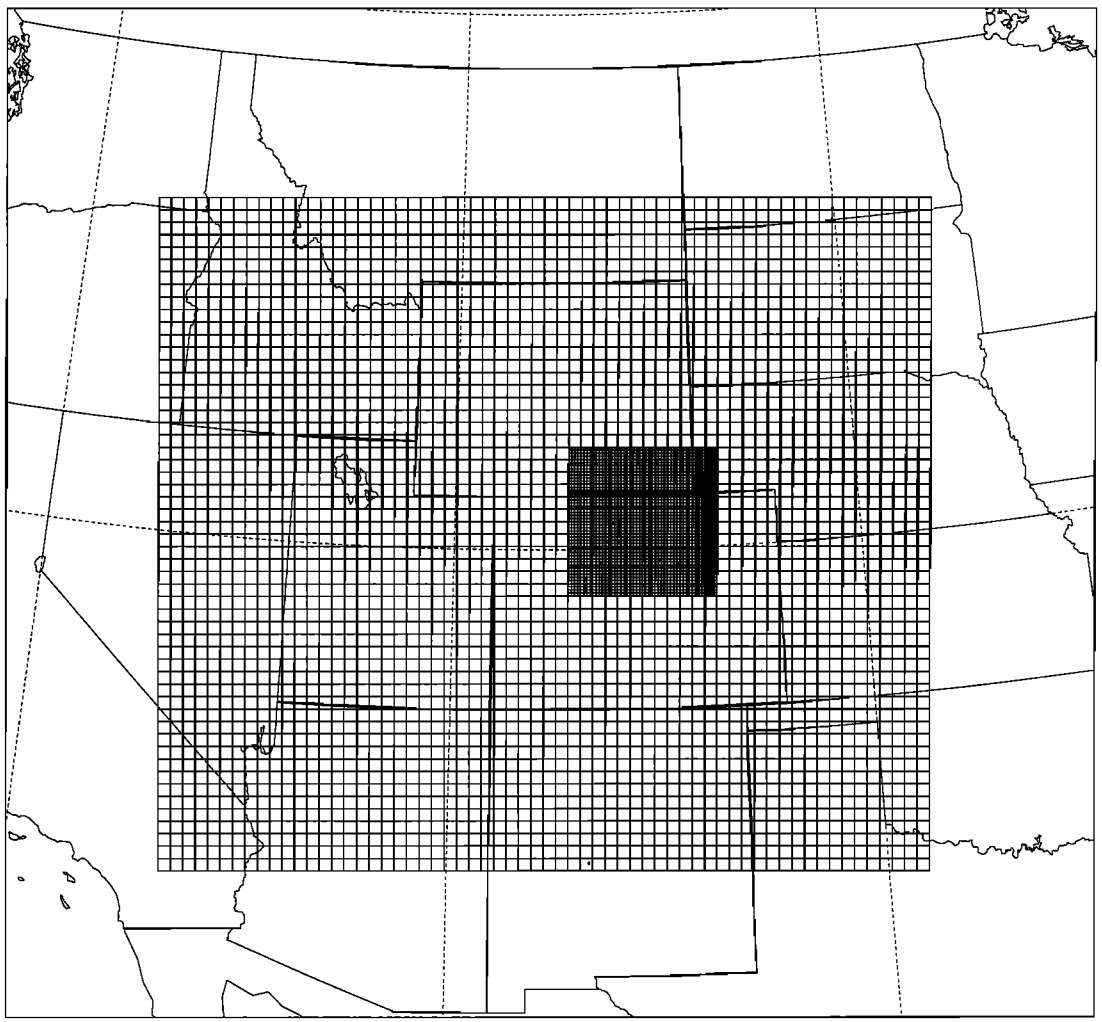

Figure 1. Domain covered by the Regional Atmospheric Modeling System two nested, interacting grids. The coarse grid interval is 24 km; the fine grid interval is 6.5 km. The fine grid is centered on Rocky Mountain National Park, Colorado.

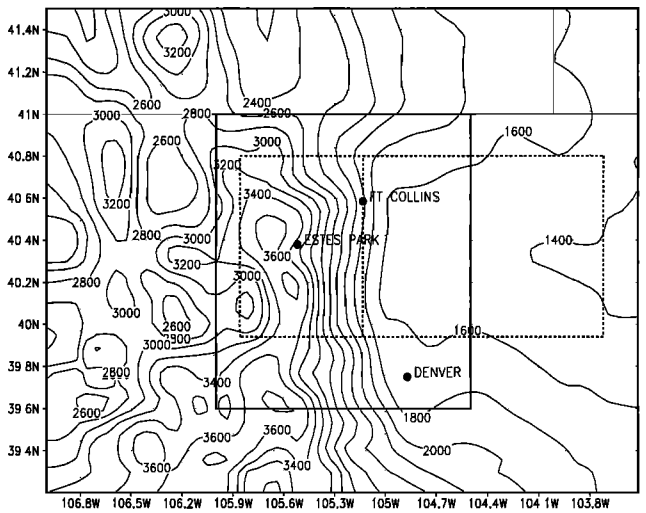

Figure 2. Topography on the fine (6.5 km) grid. Contours are by 200 m. The solid boxed region is a subdomain used in Figures 6c, 6d, 6e, and 6f. The dotted boxed region represents the subdomain used for meridional averages (discussed in text. The dotted line through Fort Collins represents the approximate division between mountains and plains regions.

simulates large-scale conditions. The finer grid covers an area of both mountain and plains in northern Colorado. The fine grid spacing used in the smaller model grid results in a realistic representation of the region's topography which is of vital importance in forcing weather features of interest (Figure 2). These topographic features include the Colorado Front Range including parts of the Continental Divide (the ridge of highest topography), intermountain valleys, and east-west topographic features such as the Cheyenne Ridge (north of Fort Collins in Figure 2) and the Palmer Divide (south of Denver in Figure 2) which are also favored regions for convective activity [*Toth and Johnson*, 1984]. These topographic features are not resolved in general circulation models or in regional climate models applied to broad domains [*Giorgi and Bates*, 1989; *Copeland et al.*, 1996] because of their relatively coarse grid spacing (~300 km and 60 km, respectively). Because of this, mountain-plains and other topographically forced regional circulations which play a large role in summer precipitation patterns in this region (as well as winter snowpack) are not accounted for explicitly nor will the mass and moisture convergence generated by these circulations be recognized by convective parameterizations in those model simulations.

Because of the fine grid spacing used in these simulations we

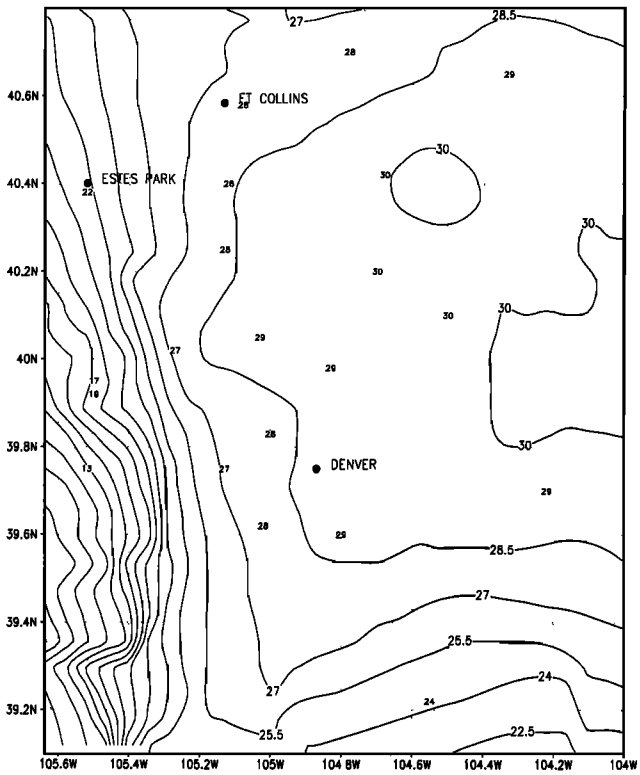

Figure 3a. Comparison of modeled average temperatures (contour by 1.5°C) with observed (Colorado mesonet) averages for afternoon (1200–1800 LST) observed temperature. Mesonet data provided by the Forecast Systems Laboratory through the Cooperative Institute for Research in the Atmosphere. Zero contour lines are omitted here, and in subsequent figures, for clarity.

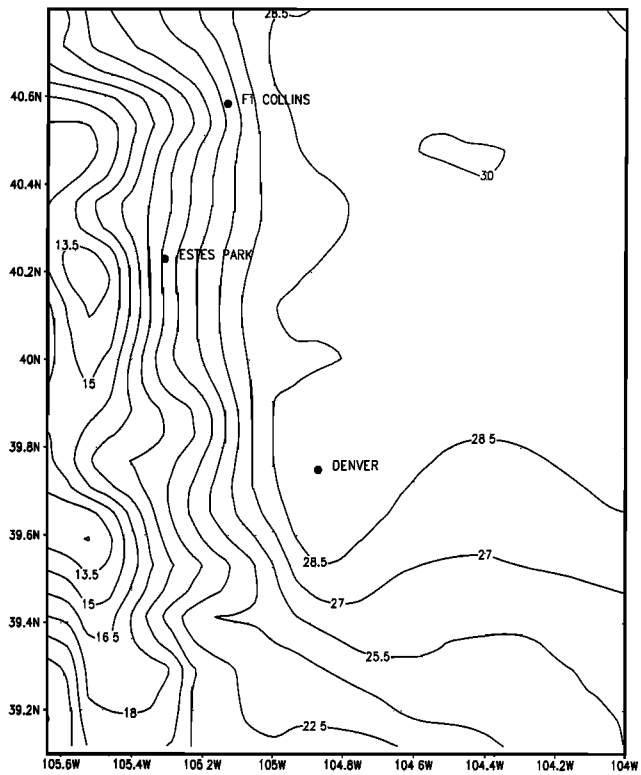

Figure 3b. Same as Figure 3a, except for afternoon (1200–1800 LST) modeled temperatures.

did not use a parameterization of convective rainfall but instead relied on resolving such disturbances through use of an explicit microphysics scheme which predicts mass mixing ratios of seven hydrometeor species including hail and graupel [*Walko et al.*, 1995]. This model configuration represents a compromise between resolved spatial scales and the ability to perform extended calculations; a 6.5-km grid allows a tractable multiday integration but is too coarse to precisely resolve most convective storms or to accurately represent their intensity. Our objective, however, is to establish sensitivity and to capture a reasonable spatial pattern of convective activity as a first approximation. Simple parameterizations of convective rainfall are not, in general, applicable to such small scales, while more complex parameterizations detract significantly from computational efficiency.

This case study was performed using three different distributions of vegetation cover in the fine grid of the model domain which represent (1) the potential natural vegetation distribution (Natural), (2) the state of land cover observed today (Current), and (3) an hypothetical distribution which increases the area of irrigated vegetation in a realistic way to represent one potential future scenario (Superirrigated). The two cases Current and Superirrigated are collectively referred to as Altered (Plate 1).

The Natural state is derived from a map of potential natural vegetation by *Küchler* [1964]. The observed state is based partially on satellite data of current land cover by the EROS Data Center [*Loveland et al.*, 1991]. In order to insure that regions not explicitly covered by an altered vegetation type (e.g., irrigated and nonirrigated farmland) were the same in all simulations, we set all cells with nonagricultural cover types in the EROS data set to the Natural state as estimated by Küchler. The EROS data were in many instances unrealistic in mountain and intermountain areas and so were ignored in favor of the Küchler estimate. The Superirrigated state (Plate 1c) was generated by filling in much of the South Platte Valley region adjacent to the mountain front with irrigated farmland so as to increase the soil moisture forcing in a potentially realistic way. This might represent an increase in irrigated cropland and urban watered landscapes associated with an increasing population and, more importantly, provides a maximally forced comparison case for assessment of signal robustness. Irrigated regions in the Superirrigated case completely occupy a region of ~1000 km by 650 km. This is on the scale of the local Rossby radius thereby providing a maximum forcing for mesoscale circulations caused solely by discontinuities in soil moisture [*Dalu et al.*,

Table 3. Comparison of Selected Surface Parameter Values for Land Use Types Which Change in These Experiments

	Albedo (Fraction)	Roughness Length, m	Initial Soil Moisture Capacity, %
Short grass	0.1/0.3	0.02	38
Dryland crop	0.1/0.3	0.06	38
Irrigated crop	0.08/0.23	0.06	75

Albedos are visible/near-infrared. From Biosphere Atmosphere Transfer Scheme (BATS) values [*Dickinson et al.*, 1993]

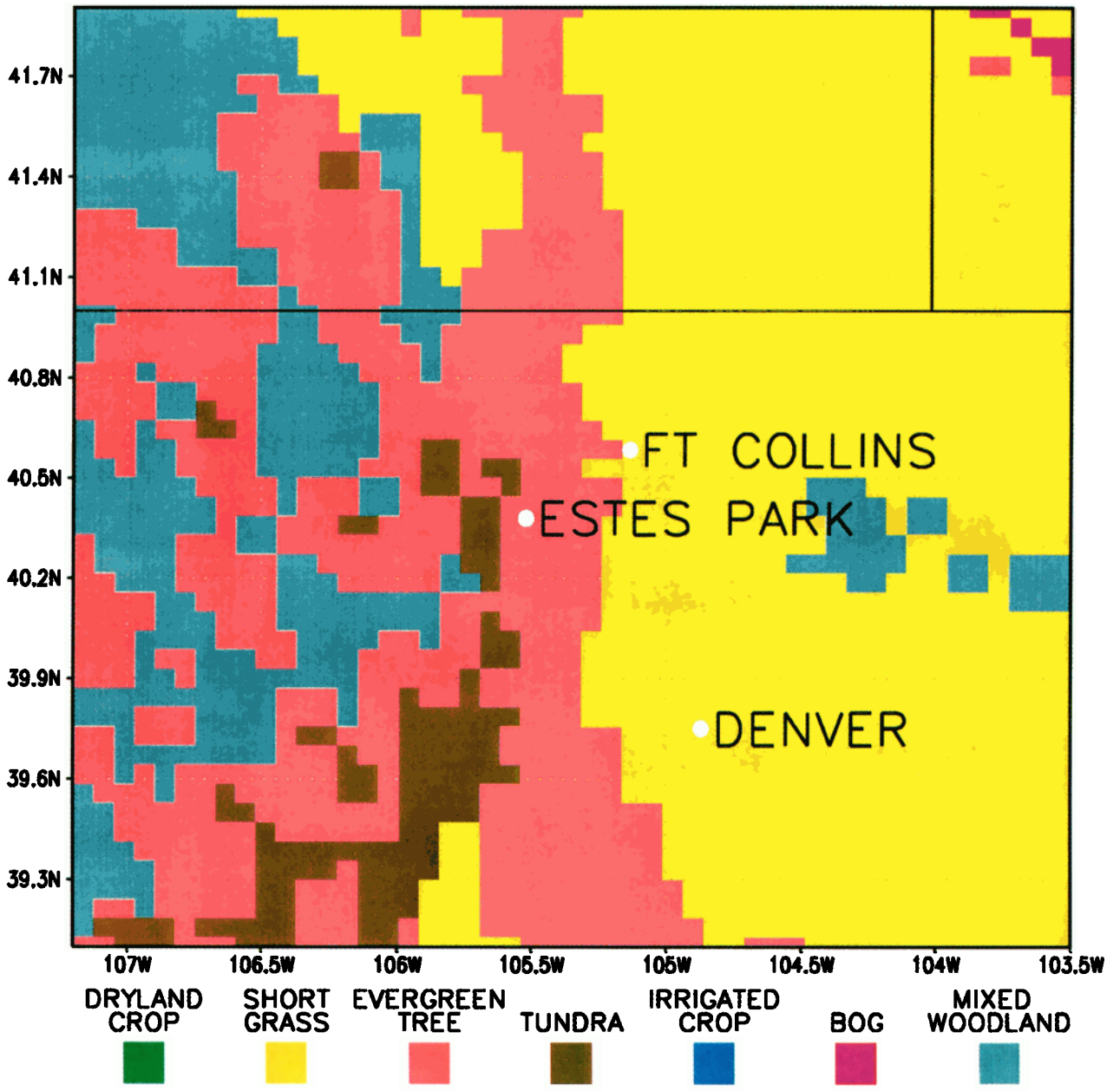

Plate 1a. Land cover types on the finest grid for the Natural case.

1996]. This type of mesoscale circulation would be expected to interact with the ambient mountain-plains circulation.

Both Altered scenarios have irrigated and nonirrigated farmland in large portions of the plains adjacent to the Rocky Mountains at the expense of shortgrass steppe. The change from short grass to agricultural land is described in the land surface model by vegetation parameters including albedo, roughness length, fractional cover of vegetation, and initial soil moisture (Table 3). The change from grassland to irrigated cropland is reflected as a change in soil moisture which was initialized at 75% of saturation for irrigated regions, while all other regions were initialized at a 38% saturation meant to represent a dry soil. Because irrigation practice in eastern Colorado generally involves a moisture treatment followed by a period of drydown, soil moisture was allowed to evolve with time during the simulation with the potential effect of removing the higher soil moisture in irrigated regions. Despite this, irrigated regions retained high relative levels of soil moisture throughout the period of integration so that moisture forcing remained relatively constant. Irrigated croplands have lower vegetation albedo and increased roughness length relative to short grassland in the vegetated fraction of the grid. Increased soil moisture also decreases the albedo of the soil fraction in irrigated regions. Finally, in areas where croplands replace short grass, roughness length is tripled. This could allow a greater transfer of heat and moisture from surface to atmosphere over the croplands due to an increase in mechanically generated turbulence. While soil type is quite variable across the mountain-plains region, a sandy-loam soil type with soil properties obtained from *Clapp and Hornberger* [1978] was assumed constant throughout the domain. Differences in soil properties in the simulation result, therefore, only from differences in soil moisture. Though we have not explicitly explored soil controls on the system, a more realistic, heterogeneous soil

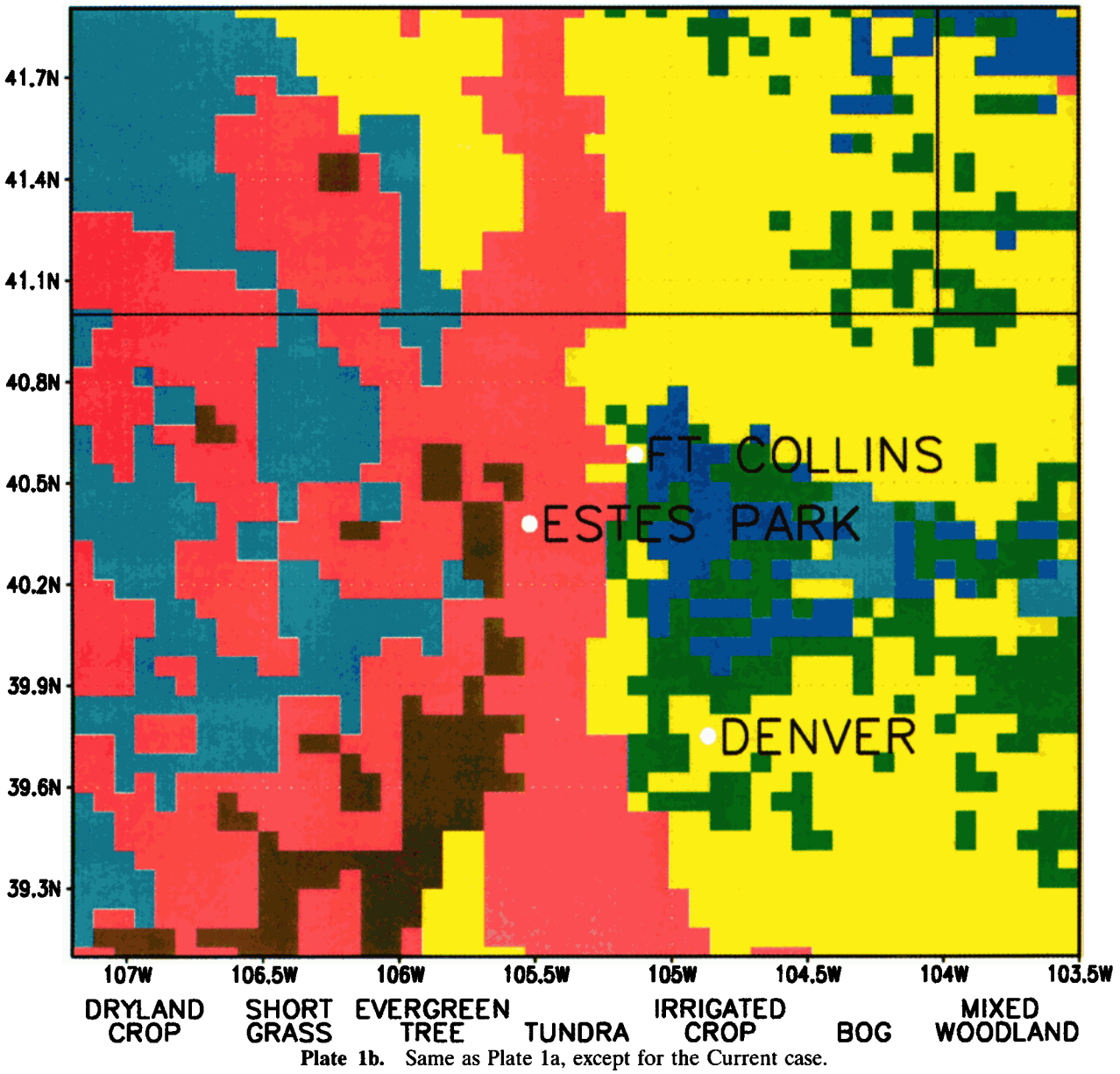

Plate 1b. Same as Plate 1a, except for the Current case.

distribution would be expected to affect soil moisture, evapotranspiration, and runoff which might, in turn, affect the horizontal temperature gradient and the circulation associated with it.

The RAMS model was initialized with, and lateral and upper boundary conditions were provided by, the National Center for Environmental Prediction upper air analyses (data formerly known as the NMC analysis) supplemented by observational data from surface stations and rawinsonde. The simulations covered a 3-day period (72 hours) from July 31 to August 2, 1992. This period was characterized by a 500 mbar ridge centered over the central United States with weak upper level flow over Colorado and weak inflow of low level and midlevel moisture from the Gulf of Mexico into the region as a result of the southwest monsoon. This is a common late summer pattern and is representative of climatological average conditions [*Toth and Johnson*, 1984]. These conditions are ideal for the development of local upslope winds in the afternoon and convergence near the Continental Divide because of the weakness of large-scale forcing. This case was characterized by weak, scattered convective activity and was chosen so that the soil moisture distributions imposed in the Altered cases was not disturbed to a marked degree (i.e., no large, organized systems over the region for long periods of time). Station data show occasional, light, scattered convective activity during this period. Between 7 and 19% of stations throughout the domain recorded light precipitation on each of the 3 days. Modeled values of daily averaged precipitation are of similar magnitude to those observed. The large-scale modeled winds, water vapor distribution, and thermal structure compare well with observed conditions for each of the three days.

Observed afternoon averaged surface air temperatures (Colorado mesonet data obtained through the Cooperative Institute for Research in the Atmosphere) are compared with the model solution in Figures 3a and 3b and show substantial

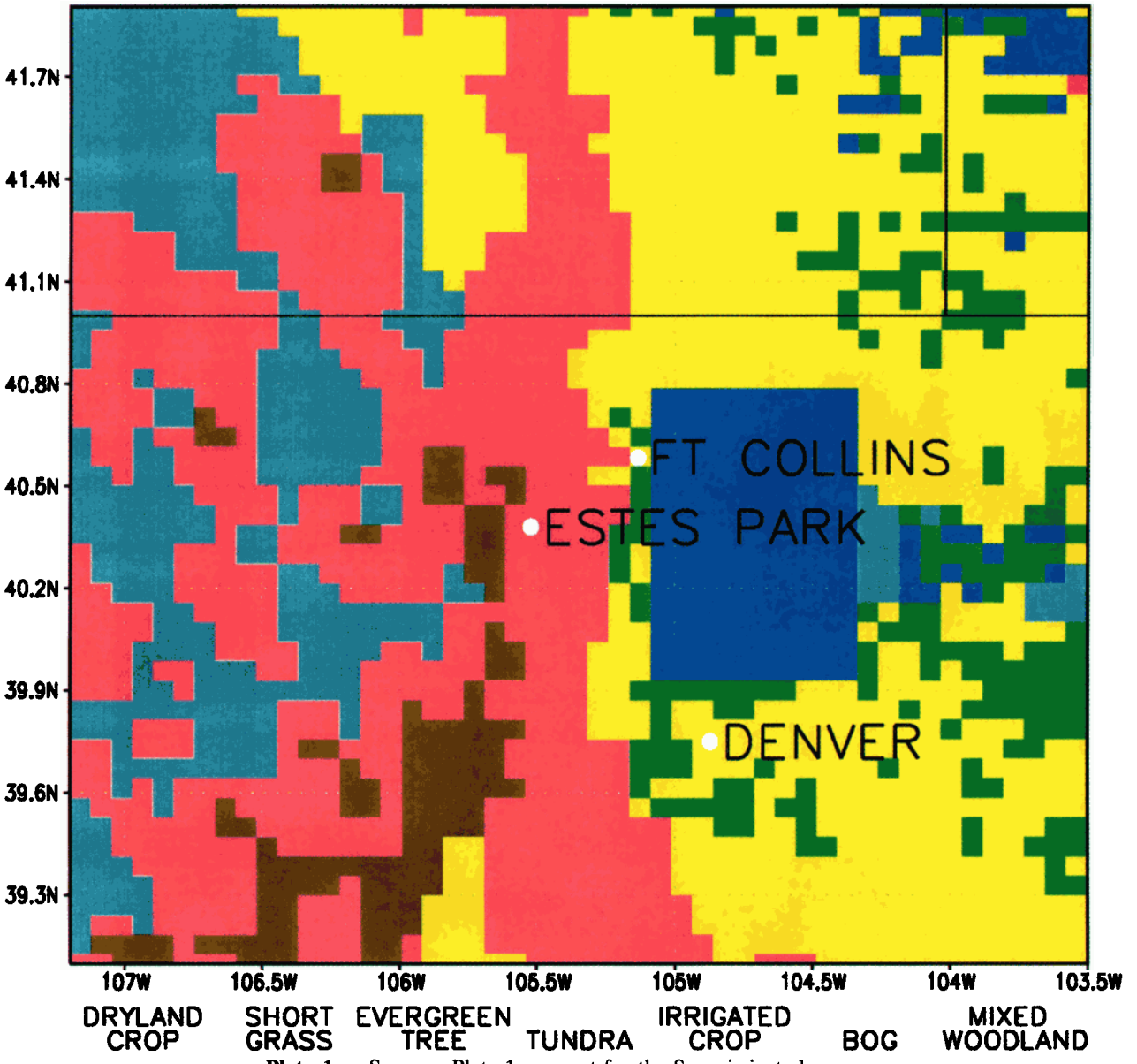

Plate 1c. Same as Plate 1a, except for the Superirrigated case.

agreement. Table 4 compares the observed diurnal cycle in temperatures with those simulated in the Current case at three sites in the domain. Denver lies on the plains, Fort Collins abuts the foothills in a transitional area, and Estes Park lies in a mountain valley on the eastern side of the Continental Divide near Rocky Mountain National Park. Differences between observed and modeled temperatures on the plains are generally within 3°C. Simulated temperatures in Estes Park are consistently cooler than observed. Model points are chosen by geographical proximity rather than terrain similarity, and model values represent an average over a 6.5 × 6.5 km (42 km^2) region. Discrepancies in observed versus simulated temperatures partially reflect the fact that in complex terrain, temperature values will differ greatly over short horizontal distances so modeled temperatures do not represent a single site in that grid.

Average dewpoints (not pictured) show reasonable spatial structure though they tend to be 1–2°C drier over the plains with a steeper than observed decrease in dew point as topography increases. For example, daily 1200 UTC dewpoint temperatures at the Denver station for the time period tend to be slightly dry in the simulations and are (observed/modeled, in °C): October 11, November 10, and August 8. On all three afternoons an easterly/southeasterly (upslope) flow developed in the simulations during the daylight hours at low levels to a maximum depth of somewhat <800 m and reversed itself at night in accordance with observed flow. Three-day average modeled easterlies ranged from 4 to 10 m s^{-1} and were slightly stronger than observed with maximum differences of 1–2 m s^{-1}.

Simulated mountain precipitation occurred mainly in association with the highest t›pography. In addition, on the third day of the simulation a large convective disturbance developed in southeastern Colorado which also occurred in the observations. Because most convective precipitation in this case is still a subgrid scale phenomenon even at this relatively high model

Table 4. Comparison of Observed Versus Simulated Temperatures at Selected Sites

	Denver		Fort Collins		Estes Park	
	obs	sim	obs	sim	obs	sim
			Maximum Temperature			
Day 1	28	27	23	23	20	16
Day 2	34	34	29	31	24	22
Day 3	31	32	31	31	26	20
			Minimum Temperature			
Day 1	14	13	10	13	10	5
Day 2	18	15	19	9	18	9
Day 3	13	18	13	20	na	12
			Average Temperature			
Day 1	21	20	17	18	15	10
Day 2	25	24	24	21	21	15
Day 3	22	25	22	25	na	16

Observed, obs; simulated, sim. In °C. Average temperatures are averaged maxima and minima; na, not available.

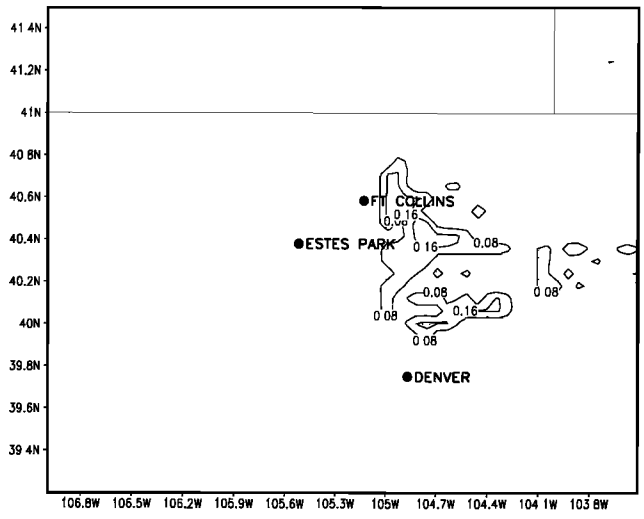

Figure 4a. Difference fields of afternoon (1200–1800 LST) averages across all 3 days; soil moisture (contour by 0.08 mm) Current minus Natural.

resolution, point comparisons with station data were not attempted.

Because of the high-resolution necessary to accurately resolve the regional circulation, we were unable to integrate for a period long enough to evaluate a climatological response or perform statistical significance tests. However, daily consistency in a diurnally forced system allows for greater confidence in the generality of the results, while the dominance of regional forcing allows us to evaluate the potential effect of land cover change on the region's summer circulation patterns.

Previous studies of topographically induced thermal circulations [*Wolyn and McKee*, 1994; *Ookouchi et al.*, 1984; *Pielke et al.*, 1991; *Poulos*, 1996] have generally used idealized topography, a horizontally homogeneous basic state, and a single day or less of simulation and so have not investigated with several realizations impacts both on the plains and at higher elevations under realistic initial and boundary conditions, this is our goal here.

5. Results

5.1. Spatial and Temporal Averages

In order to minimize daily variations in the signal which may not be representative of general behavior we present results as averages over the 3-day period. All anomalies are presented relative to the Natural case. We compared the Altered and Natural simulations in terms of their averages over afternoon hours (1200–1800 LST) on all 3 days. These times represent the period when the mountain-plains circulation was most developed and mountain convection most active.

Soil moisture in the top, 2-cm-deep, soil layer (Figures 4a and 4b) was greater in the two Altered simulations consistent with initial conditions for the irrigated lands. Latent heat fluxes (Figures 4e and 4f) were larger over large areas in the plains to maximum values of 160–180 W m^{-2} in the two Altered cases, while sensible heat fluxes (Figures 4c and 4d) were lower over moist soils (maximum decreases were ~150 W m^{-2} in both Altered cases). The additional moisture supplied to the plains boundary layer at the expense of sensible heating represented the main driver for subsequent dynamical changes. Larger sensible heat fluxes just to the west of the irrigated regions as well as near the eastern grid boundary occur in similar magnitude in both Altered cases. These increased sensible heat fluxes are partially a result of more efficient transport of heat to the atmosphere due to the large roughness length of the dryland cropping occupying those areas relative to the natural grasslands. The higher moisture content of air downstream from the irrigated regions would also act to enhance sensible heating in this region through suppression of latent heating. These effects emphasize the complicated and sometimes competing atmospheric forcings inherent in changing land cover.

The Altered cases had cooler lower atmospheres (0–640 m; though because this layer is well mixed, these are indicative of surface air temperatures as well) over the regions of enhanced soil moisture of nearly 0.7° in the Current case and almost 1.0° in the Superirrigated case relative to the Natural case (Figures 5a and 5b). Owing to the advection of colder air from the plains, this cooler air is seen far up the eastern slope of the mountain front in both Altered cases, especially in the Superirrigated case (refer to topography in Figure 2).

The cooler plains and mountains in the Altered cases caused

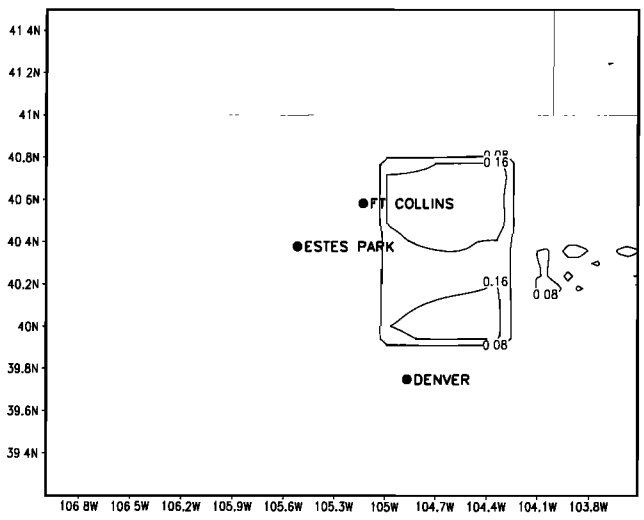

Figure 4b. Same as Figure 4a, except for soil moisture (contour by 0.08 mm) Superirrigated minus Natural.

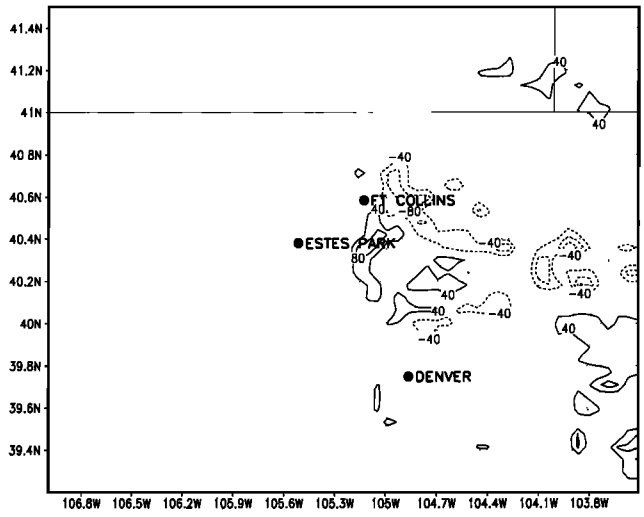

Figure 4c. Same as Figure 4a, except for sensible heat flux (contour by 40 W m^{-2}) Current minus Natural.

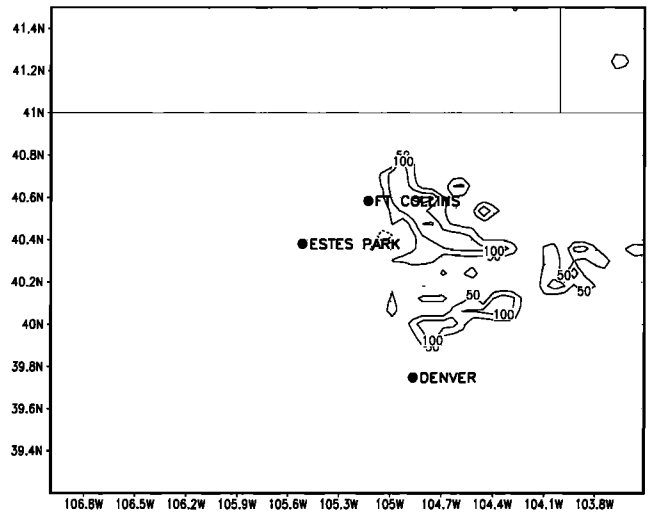

Figure 4e. Same as Figure 4a, except for latent heat flux (contour by 50 W m^{-2}) Current minus Natural.

decreased easterly upslope winds in the same regions due to the lower sensible heating of the atmosphere and reduced pressure gradient (Figures 5e and 5f). The plains are on a slope themselves, and so the large cooling at the base and up the eastern slopes of the Rockies substantially reduced upslope flow from points farther east. The maximum wind reduction, represented by positive anomalies in Figures 5e and 5f due to easterly (negative) ambient wind direction (average U winds in the Natural case are provided in Figure 5g for locations of easterly and westerly flow), was more than 1.5 m s^{-1} in the Current case and nearly 2 m s^{-1} in the Superirrigated case relative to the Natural case. The decreased easterlies extended to high elevations in both Altered cases.

The presence of irrigated land was also reflected in low level atmospheric moisture differences where dewpoint temperatures increased in the northern part of the irrigated regions in the two Altered cases (Figures 5c and 5d). This northward shift is a reflection of a southerly wind component which advected moisture slightly to the north. In the Current case, dewpoint temperature was slightly lower to the west of the center of the irrigated region and at higher elevations as a result of flow patterns which moved dry air in from the south. This had impacts on mountain cloud cover and convection.

The higher low level moisture in the Altered simulations relative to the Natural case caused larger convective available potential energy (CAPE) in the region just north of Fort Collins by ~100–150 J kg^{-1} in both cases despite cooler temperatures (Figures 6a and 6b). Diminished CAPE in the Current case south of Fort Collins resulted from lower temperature and less moisture in the area. In the Superirrigated case a smaller decrease in CAPE occurs south of Fort Collins, while a sizeable increase in CAPE occurs at higher elevations between Fort Collins and Estes Park owing to enhanced upslope advection of moisture from the irrigated regions in spite of decreased easterly flow (Figure 5f).

Figures 6c and 6d display the precipitation differences for a subset of the region focusing on higher elevations and the mountain-plains transition (solid boxed region in Figure 2).

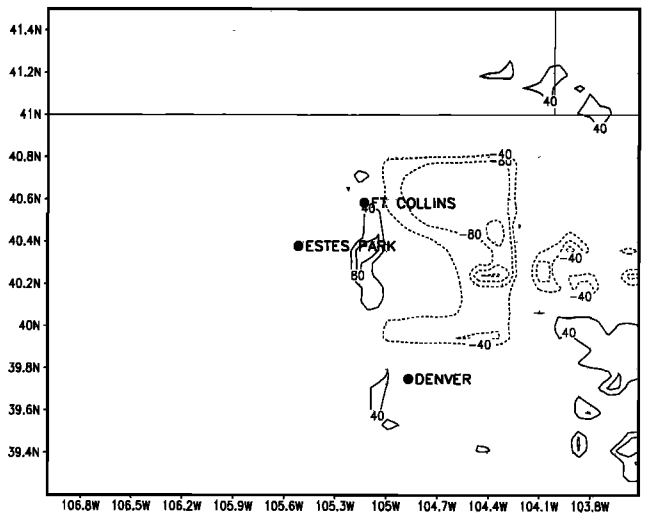

Figure 4d. Same as Figure 4a, except for sensible heat flux (contour by 40 W m^{-2}) Superirrigated minus Natural.

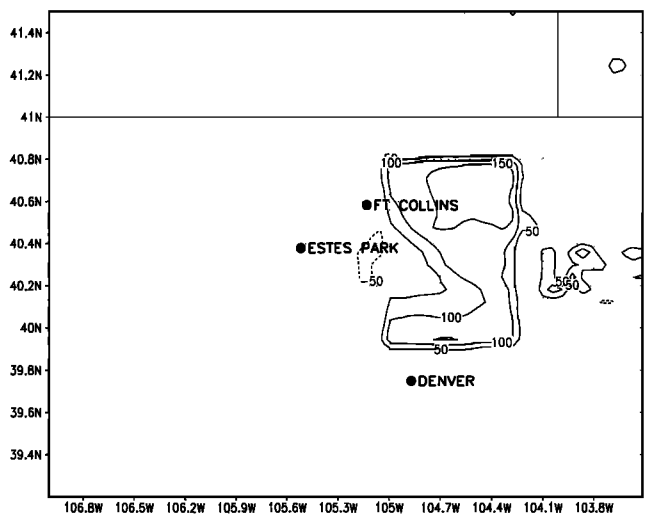

Figure 4f. Same as Figure 4a, except for latent heat flux (contour by 50 W m^{-2}) Superirrigated minus Natural.

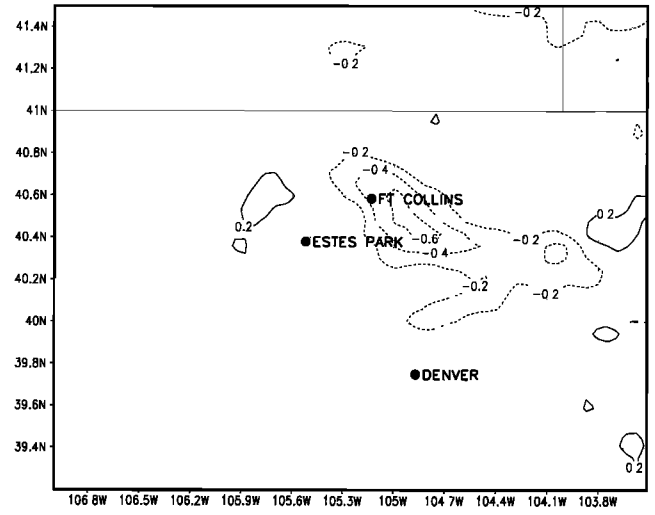

Figure 5a. Fields averaged vertically from 0 to 640 m (first five model layers) and over afternoon hours (1200–1800 LST); temperature difference (contour by 0.2°C) Current minus Natural.

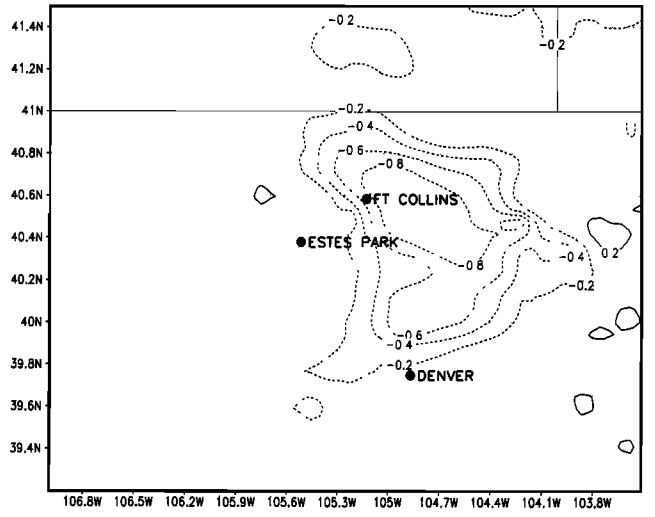

Figure 5b. Same as Figure 5a, except temperature difference (contour by 0.2°C) Superirrigated minus Natural.

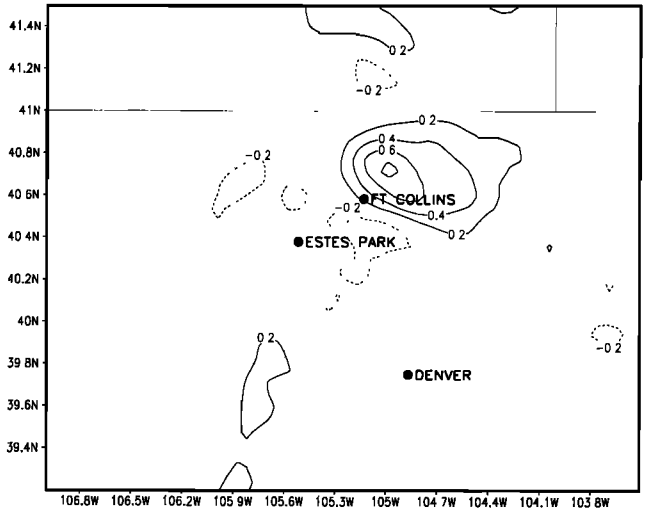

Figure 5c. Same as Figure 5a, except dewpoint temperature difference (contour by 0.2°C) Current minus Natural.

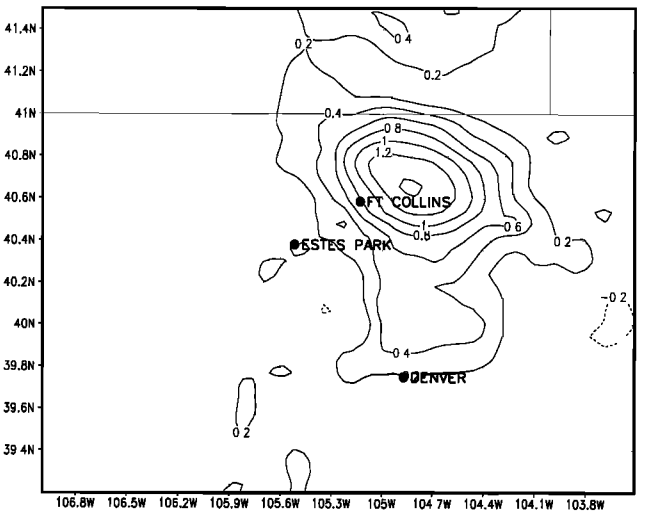

Figure 5d. Same as Figure 5a, except dewpoint temperature difference (contour by 0.2°C) Superirrigated minus Natural.

Total accumulated rainfall was affected west of areas with altered land cover, including the transitional region between mountain and plains and at highest elevations. A precipitation increase occurred in the area of Fort Collins in both Altered cases, while two minima occurred at high elevations, one to the north and one to the south of Estes Park. These features are similar in both Altered cases, though anomalies are of higher magnitude in the Superirrigated case.

The total condensate field differences, also presented for the solid boxed region in Figure 2, reflecting changes in cloud cover, had a series of positive and negative anomalies in a north-south line along the Continental Divide reflecting an orderly arrangement of preferred areas of cloudiness (Figures 6e and 6f). Anomalies were spatially similar in each Altered case but were of stronger magnitude in the Superirrigated case than in the Current case.

As an indication of the daily extent of regions affected by land use changes in the plains, standard deviations of after-

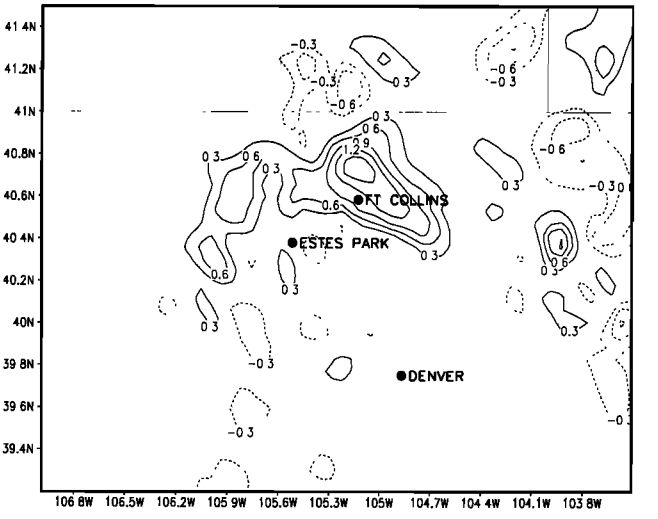

Figure 5e. Same as Figure 5a, except east-west wind difference (contour by 0.3 m s^{-1}) Current minus Natural. Positive anomaly values represent decreases in easterly flows or increased westerlies relative to the Natural case.

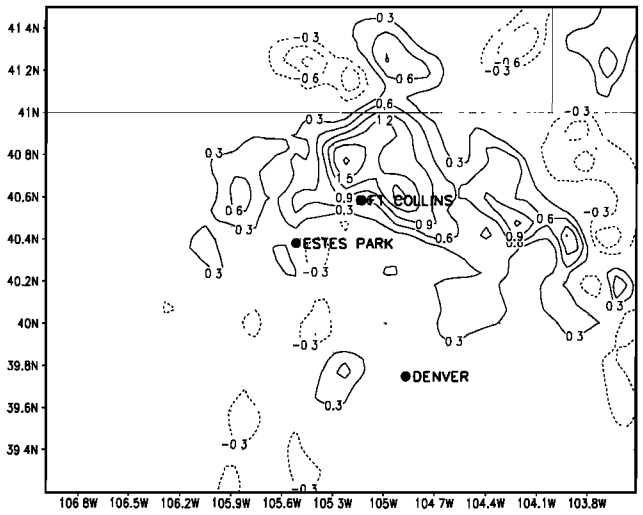

Figure 5f. Same as Figure 5a, except east-west wind difference (contour by 0.3 m s^{-1}) Superirrigated minus Natural. Positive anomaly values represent decreases in easterly flows or increased westerlies relative to the Natural case.

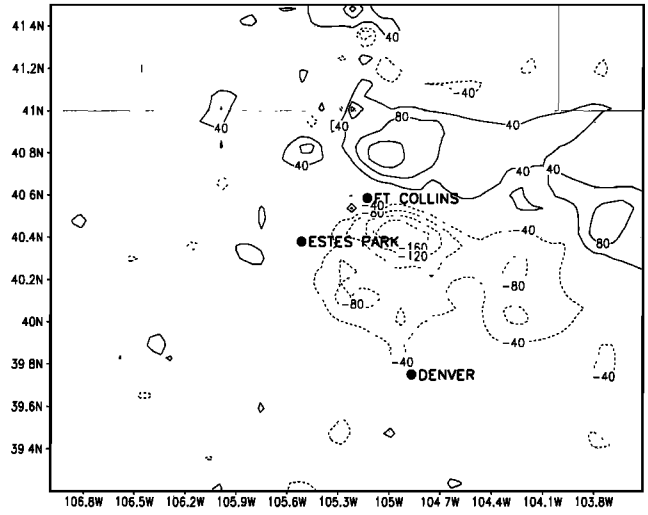

Figure 6a. Difference fields averaged vertically from 0 to 640 m (first five model layers) and over afternoon hours (1200–1800 LST); CAPE (contour by 40 J kg^{-1}) Current minus Natural.

noon averaged temperature, and dewpoint temperature differences (Current minus Natural) are provided in Figures 7a and 7b, which show that the effect of these land use changes can penetrate into the mountains on individual days. The effect is similar but stronger in the Superirrigated case differences (not shown).

5.2. Meridional Averages

To provide a picture of east-west structure, we took north-south averages over a subdomain where surface forcing mechanisms were strongest and were expected to have the greatest impact (see dotted box in Figure 2). This region includes the largest irrigated regions on the plains and continues west past the highest topography.

The afternoon divergent maximum in the first 640 m of the atmosphere (Figure 8a, at approximately grid points 27–29) and the weak divergence at most points farther east increased in each of the Altered cases, while in the mountains, less convergence occurred along the lower slope of the mountains (grid points 24 to 25) in the Altered cases as well as at the convergent maximum at grid point 21. Vertical velocity (not pictured) was correspondingly slightly lower in these regions in both Altered cases.

Meridionally averaged daily precipitation (Figure 8b) showed a spatially complicated response. Less precipitation fell on the eastern boundary of the domain was due to southern shifts of a precipitation center in both Altered cases which moved it outside the averaging area. A plains maximum occurred in the Superirrigated case centered at the boundary between wet and dry soils (grid point 39), which developed as a result of a weak circulation generated at the discontinuity. The greater precipitation at the boundary between wet and dry regions in this case would be expected to diminish the thermal contrast here and therefore act as a first-order negative feedback. It is unclear how this feedback would exhibit itself in the

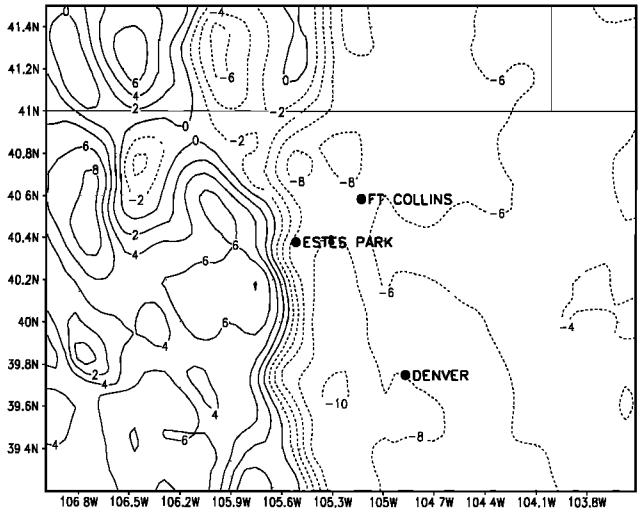

Figure 5g. Same as Figure 5a, except undifferenced east-west winds in the Natural case provided for orientation of easterlies and westerlies (contour by 2.0 m s^{-1}).

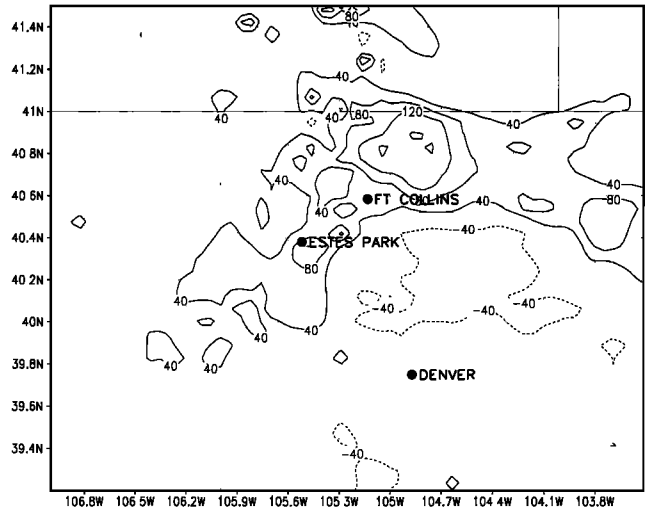

Figure 6b. Same as Figure 7a, except for CAPE (contour by 40 J kg^{-1}) Superirrigated minus Natural.

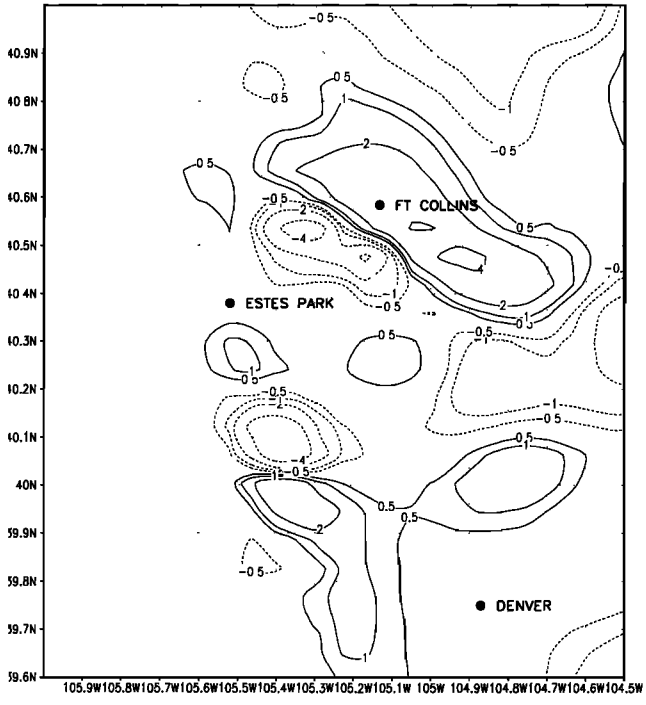

Figure 6c. Same as Figure 7a, except for mountain precipitation (contour by 0.5, 1.0, 2.0, 4.0, 8.0 mm d^{-1}) Current minus Natural.

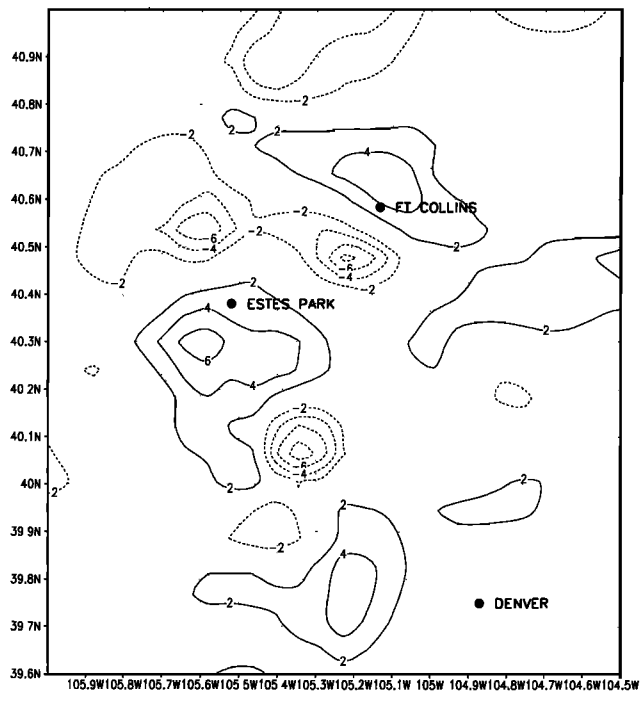

Figure 6e. Same as Figure 7a, except for mountain vertically integrated condensate (contour by 2 kg) Current minus Natural.

long term, though it emphasizes the potential for both positive and negative feedback effects due to changes in precipitation amount and distribution. The rainfall maximum in the mountains, somewhat east of the convergent maximum (Figure 8a) due to advection of storms by ambient westerlies, was smaller in both Altered cases consistent with smaller convergence. The rainfall maximum in the Current case had a broader areal distribution relative to the Natural case. The Superirrigated case had a narrower precipitation distribution and less precipitation both in the mountains and in lower elevations near the mountains relative to the Natural case.

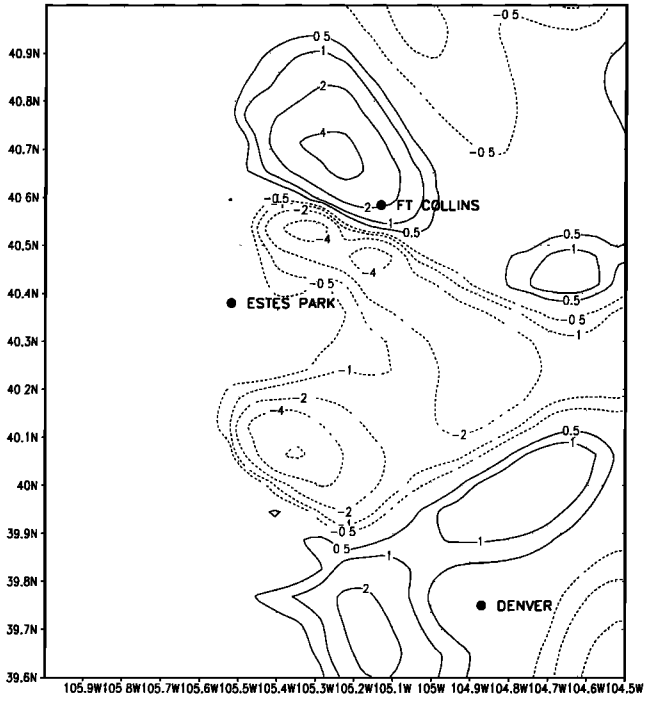

Figure 6d. Same as Figure 7a, except for mountain precipitation (contour by 0.5, 1.0, 2.0, 4.0, 8.0 mm d^{-1}) Superirrigated minus Natural.

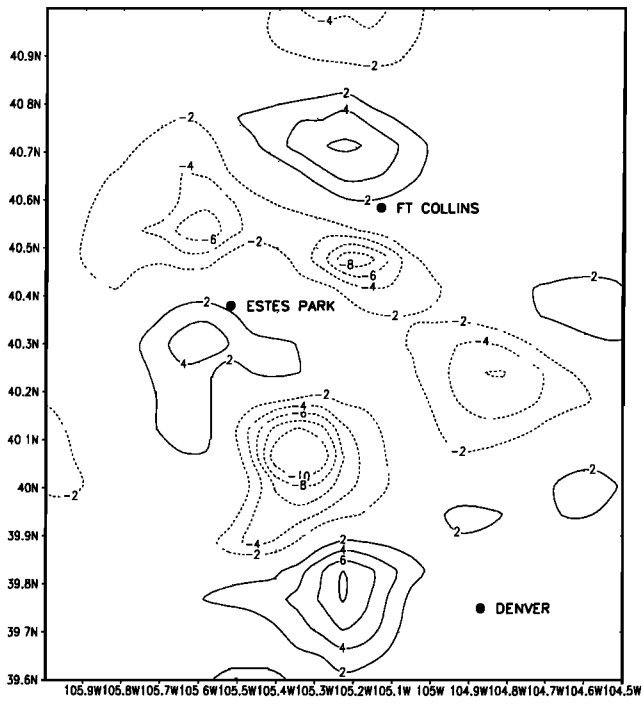

Figure 6f. Same as Figure 7a, except for mountain vertically integrated condensate (contour by 2 kg) Superirrigated minus Natural.

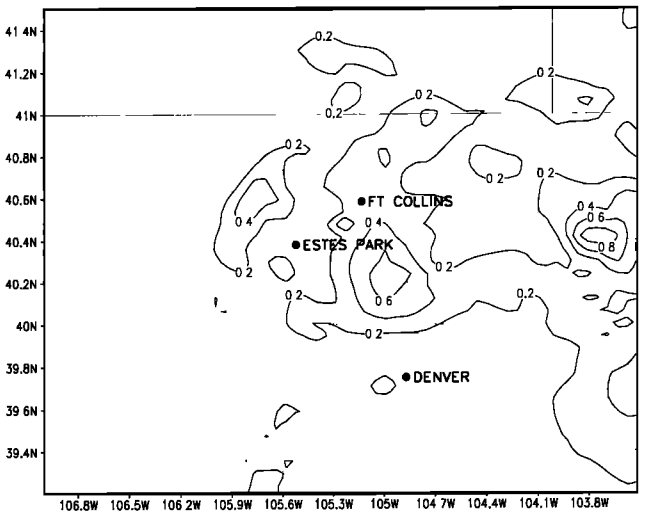

Figure 7a. Standard deviation of differences in time. Differences were averaged vertically from 0 to 640 m (first five model layers) and over afternoon hours (1200–1800 LST); temperatures (contour by 0.2°C) Current minus Natural.

Total condensate integrated throughout the atmosphere and averaged daily is a proxy for average cloud cover in the region (Figure 8c). Meridionally averaged condensate increased over most of the plains in the Altered cases with a secondary maximum in the Superirrigated case paralleling the precipitation field. The condensate maximum at high elevations was larger in the Current case but smaller in the Superirrigated case. We emphasize that variables such as precipitation and condensate had highly variable spatial responses to the relatively consistent dynamic and thermodynamic forcings and their distribution were highly sensitive to the chosen averaging domain.

6. Sensitivity to Added Model Complexity

The basic numerical model described above is unrealistic in several respects. Two obvious areas are in the use of a simple radiative parameterization and a constant leaf area index (LAI) between vegetation types. In an effort toward building a more comprehensive model of the effects of land use change in this region, we explored the total response by adding each of these effects individually on top of land use changes described earlier. We performed two sensitivity studies which covered the first 12 hours of the original 3-day period. The first used a more accurate radiation parameterization which also allows for radiative interaction with clouds [*Harrington*, 1997]. In a second study we doubled green leaf area from 1.0 to 2.0 m^2/m^2 in agricultural areas to represent the increase in this parameter in observed systems. These results are shown in Figure 9. We compare Figures 9a–9c simply to indicate sensitivity and to

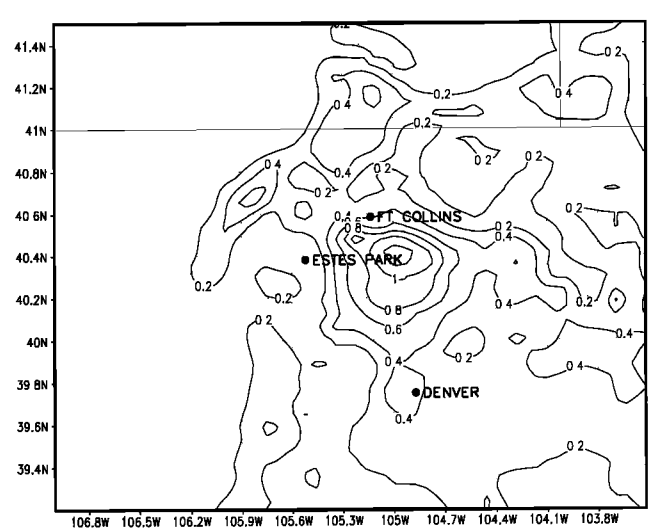

Figure 7b. Same as Figure 7a, except for dewpoint temperatures (contour by 0.2°C) Current minus Natural.

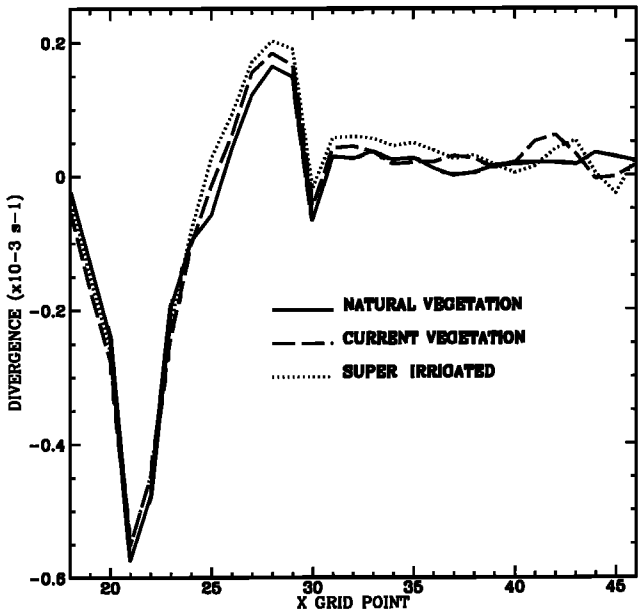

Figure 8a. Comparison of north-south averages over dotted box in Figure 2 for the three cases; 1200–1800 LST divergence (s^{-1}) 0–640 m.

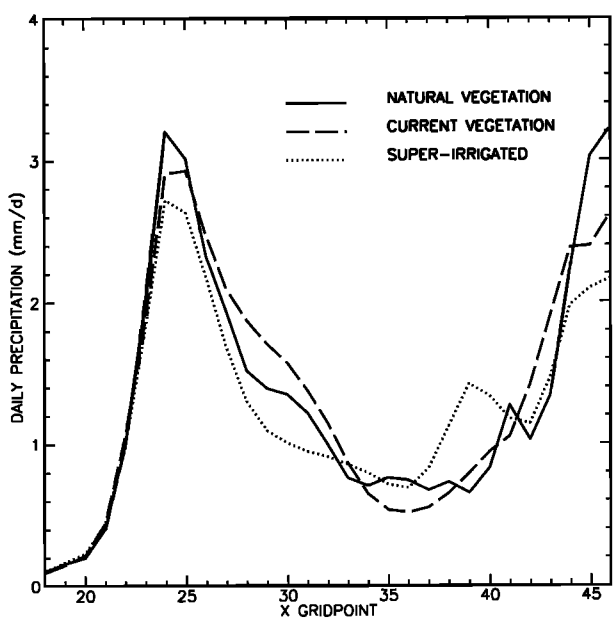

Figure 8b. Same as Figure 8a, except for total daily precipitation (mm d^{-1}).

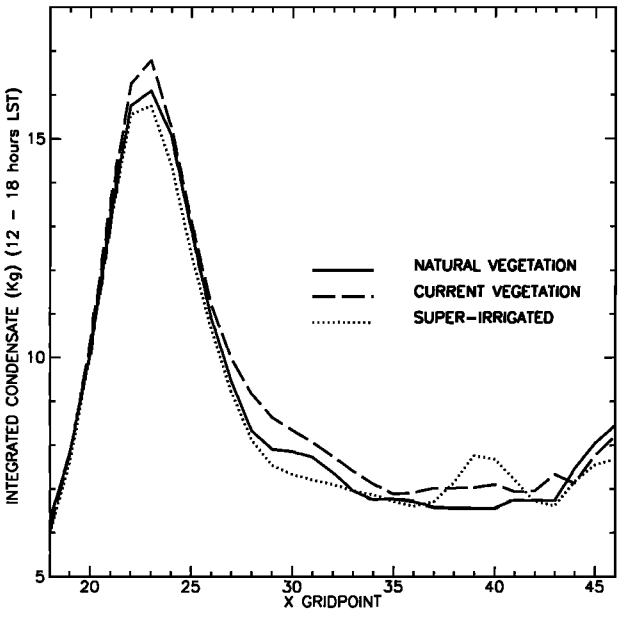

Figure 8c. Same as Figure 8a, except for daily vertically integrated condensate (kg) (solid and liquid). The mountain region approximately occupies grid points 18–28, while the plains region occupies grid points 29–46.

highlight the complexity of the issues involved. We do not examine the response in detail.

Figure 9a shows the temperature difference between the Current and Natural cases for the hours 1200–1800 LST on the first day of simulation. As a comparison, Figure 9b shows the same field except with the alternative radiation scheme implemented. The temperature response with the alternative radiation covers a larger area than in the original simulation and has a larger maximum temperature decrease which more than doubled. Similarly, a comparison in a case where agricultural LAI is doubled (Figure 9c) also strengthened the initial response by >50% and broadened the area affected.

These changes in plains temperature affected the magnitude

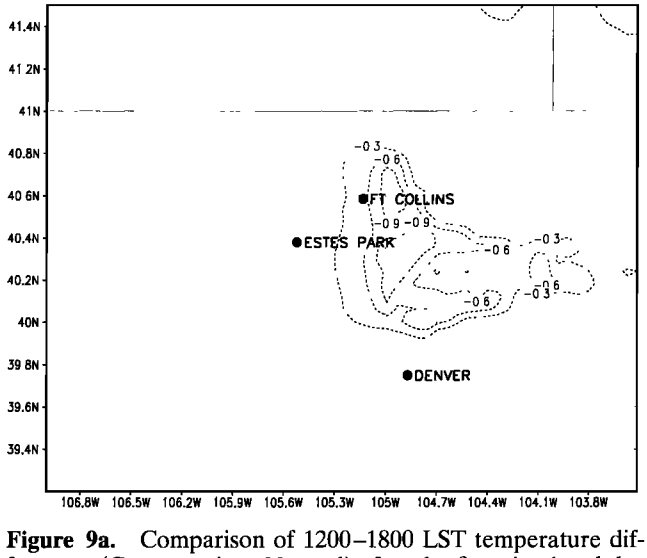

Figure 9a. Comparison of 1200–1800 LST temperature differences (Current minus Natural) after the first simulated day averaged vertically from 0 to 640 m.

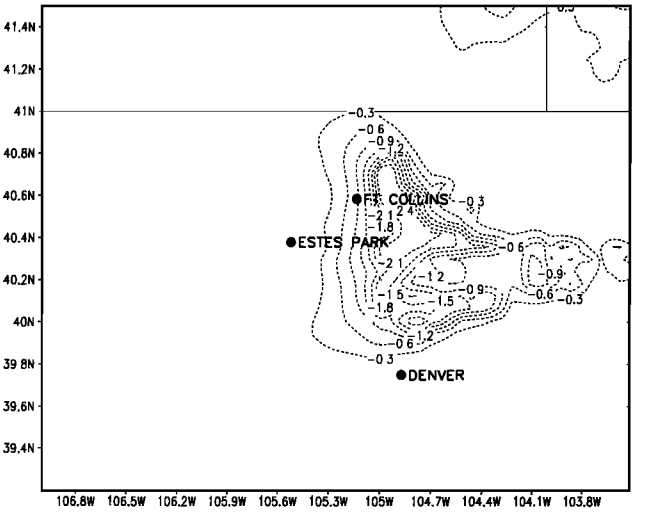

Figure 9b. As in Figure 9a but with the two-stream radiation scheme included in both simulations.

of the mountain-plains breeze where the afternoon easterly winds (not shown) slowed by up to 2.8 m s^{-1} in the Current case with the alternate radiation scheme and up to 2.4 m/s in the Current case with doubled LAI. The largest difference in the original model was 1.2 m s^{-1} on this day. Changes in the mountains-plains breeze of this magnitude would be expected to have further impacts on cloud cover and precipitation as indicated in the calculations of section 3.

7. Discussion and Conclusions

Experiments with a regional atmospheric model with explicit representation of natural, present day, and a hypothetical, future land-cover distribution were performed in the region of Rocky Mountain National Park in northern Colorado. These experiments showed important effects on atmospheric dynamics, thermal structure, and hydrology in both the plains and adjacent mountains. Effects on the mountain-plains circulation induced by changes in land use were of sufficient magnitude to affect cloud cover, precipitation, surface hydrology, and tem-

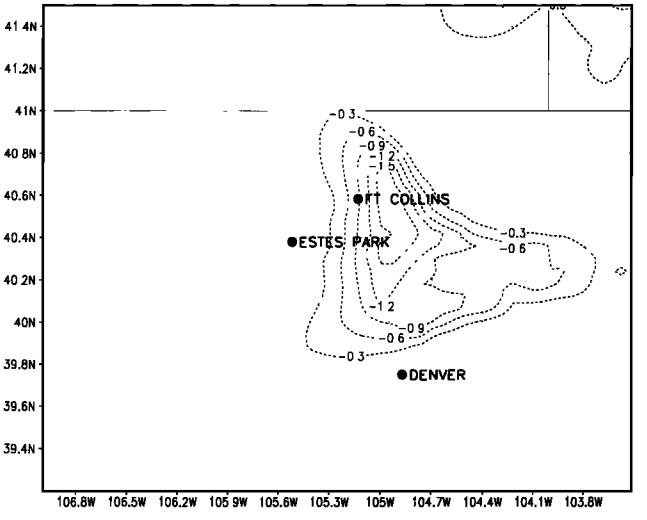

Figure 9c. As in Figure 9a but with increased green leaf area in agricultural areas in both simulations.

perature at higher elevations. The responses in the temperature and wind fields were proportionately stronger in the Superirrigated case than the Current case, indicating a monotonic response to surface forcing which was relatively linear. Behavior of the components of the hydrological cycle, especially when considering remote effects, was highly nonlinear, however, so that perturbations varied widely between scenarios.

Some responses had, however, daily consistency over the course of the 3-day simulation and between the two cases where altered vegetation was present (Current and Superirrigated cases). Compared to the Natural case, the effects of altered land cover in the plains included smaller sensible heat fluxes over moist regions, larger latent heat fluxes over moist regions, cooler boundary layer during the day, and more low level moisture. These changes altered the mesoscale flow dynamics leading to the following responses: diminished easterly low level afternoon flow over a wide area, less low-level afternoon convergence in the mountains in the subdomain presented in section 5, cooler eastern slope mountain regions, and precipitation and cloud cover, nonlinearly affected in magnitude and spatial pattern in both plains and mountain regions.

Though true significance testing cannot be run on such short simulations, confidence in the trends in the results was enhanced by daily consistency over the 3 days. These simulations also confirmed the predictions of a simple analytic model (section 3) that temperature changes due to plains irrigation and other land cover changes can have large effects on the local dynamic response, which in turn affects the hydrologic response which was communicated to higher elevations remote from actual land use changes. These mountain regions have sharply defined vegetative zones in which species and ecological processes are strongly affected by temperature, soil moisture, and insolation. Therefore responses may be larger when feedbacks due to vegetation changes (which may already be occurring [*Stohlgren et al.*, 1998]) are included.

The sensitivity studies reported in section 6 suggest that radiation characterization as well as the details of other processes such as vegetation physiology are likely to be important to simulating climate change in northeastern Colorado and that reasonable depictions of each must be included simultaneously in order to more thoroughly investigate the sensitivity of weather and climate to landscape structure. Because these effects are related in nonlinear ways, it would be a mistake to conclude that the temperature effects are additive. However, both sensitivity studies significantly enhanced the original signal both in magnitude and area which suggests our original model results may be underestimating the impact of observed land use change during this simulated period in both magnitude and spatial extent. One potential source of uncertainty which we have not completely accounted for is our ability to simulate convective precipitation. While the details of the convective response are uncertain because we are not precisely resolving either the terrain or the individual storms, we believe the gross features are likely to be realistic because of the strong topographic forcing and the realistic east-west occurrence of convergent zones.

Observed and inferred temperature trends in this region are also suggestive of the responses seen in these simulations. Analysis of observations shows a general regional cooling in July which is distinct from temperature changes at larger geographic scales. The simulations reported here show decreased afternoon temperatures and changes in cloudiness and precipitation in remote areas which could signal broader-scale and longer-term responses. While we have chosen a time period which is representative of climatological conditions, it is unclear how these hydrological effects might express themselves in a long-term climatology. This regional temperature decrease and the fact that observed temperature responses at high elevation stations are highly variable in space suggest that there are local climate controls at work. We have demonstrated that one such control may be land use change which may need to be accounted for in the climate record [e.g., *Pielke et al.*, 1998]. However, it is unlikely that this is the only control. More complete models combined with climatological-length simulation periods and closer evaluation of climate records and surrogate measurements will be necessary to understand the effects of changing climate at all scales in the Colorado Rocky Mountains and other similar plain systems.

Appendix

Stations in the Southwest United States are Colorado, New Mexico, Utah, and Arizona. The southeast Colorado stations are Eads, Holly, Lamar, Las Animas, and Rocky Ford. The western Colorado stations are Collbran, Cortez, Crested Butte, Delta, Dillon, Glenwood Springs, Grand Junction, Gunnison, Hayden, Montrose, Rifle, Silverton, Telluride, and Spicer. The northeastern Colorado stations are Burlington, Boulder, Byers, Estes Park, Fort Collins, Fort Morgan, Holyoke, Parker, Stratton, and Wray.

Acknowledgments. The authors acknowledge support from the National Park Service (NPS) and the National Biological Survey (NBS) grants CEGR-R92-0193 and COLR-R92-0204, U.S. Geological Survey (USGS) grant 1434-94-A-01275, EPA grant R824993-01-0, and the National Oceanic and Atmospheric Administration (NOAA) grant NA36GP0378. Additional support was received from the University Corporation for Atmospheric Research Climate Systems Modeling Program contract UCAR S9361 and the Niwot Ridge Long-Term Ecological Research (LTER) Project (funded by the National Science Foundation, NSF). The National Center for Atmospheric Research is sponsored by NSF. Our thanks to John Knaff, Cathy Finley, Dallas McDonald, and the anonymous reviewers for substantive and editorial comments. Our thanks also to Nan McClurg and the Cooperative Institute for Research in the Atmosphere (CIRA) for assistance with the mesonet data.

References

Atkinson, B. W., *Meso-scale Atmospheric Circulations*, Academic, San Diego, Calif., 1981.

Avissar, R., Recent advances in the representation of land-atmosphere interactions in general circulation models, *U.S. Natl. Rep. Int. Union Geod. Geophys. 1991–1994*, *Rev. Geophys.*, *33*, 1005–1010, 1995.

Barnston, A. G., and P. T. Schickedanz, The effect of irrigation on warm season precipitation in the southern Great Plains, *J. Clim. Appl. Meteorol.*, *23*, 865–888, 1984.

Baron, J. S., M. D. Hartman, T. G. F. Kittel, L. E. Band, D. S. Ojima, and R. B. Lammers, Effects of land cover, water redistribution, and temperature on ecosystem processes in the South Platte Basin, *Ecol. Appl.*, *6*, 1037–1051, 1998.

Beebe, R. C., Large scale irrigation and severe storm enhancement, paper presented at Symposium on Atmospheric Diffusion and Air Pollution, Am. Meteorol. Soc., Santa Barbara, Calif., 1974.

Bluestein, H., *Synoptic-Dynamic Meteorology in Midlatitudes*, 431 pp., Oxford Univ. Press, New York, 1992.

Bonan, G. B., D. Pollard, and S. L. Thompson, Effects of boreal forest vegetation on global climate, *Nature*, *359*, 716–718, 1992.

Charney, J. G., W. J. Quirk, S. H. Chow, and J. Komfield, A comparative study of the effects of albedo change on drought in semi-arid regions, *J. Atmos. Sci.*, *34*, 1366–1385, 1977.

Chase, T. N., R. A. Pielke, T. G. F. Kittel, R. Nemani, and S. W.

Running, The sensitivity of a general circulation model to large-scale vegetation changes, *J. Geophys. Res.*, *101*, 7393–7408, 1996.
Clapp, R. B., and G. M. Hornberger, Empirical equations for some soil hydraulic properties, *Water Resour. Res.*, *14*, 601–604, 1978.
Copeland, J. H., R. A. Pielke, and T. G. F. Kittel, Potential climatic impacts of vegetation change: A regional modeling study, *J. Geophys. Res.*, *101*, 7409–7418, 1996.
Cotton, W. R., and R. A. Pielke, *Human Impacts on Weather and Climate*, 288 pp., Cambridge Univ. Press, New York, 1995.
Dalu, G. A., R. A. Pielke, M. Baldi, and X. Zeng, Heat and momentum fluxes induced by thermal inhomogeneities, *J. Atmos. Sci.*, *53*, 3286–3302, 1996.
Dickinson, R. E., Land-atmosphere interaction, *U.S. Natl. Rep. Int. Union Geod. Geophys., 1991–1994, Rev. Geophys.*, *33*, 917–922, 1995.
Dickinson, R. E., A. Henderson-Sellers, and P. J. Kennedy, Biosphere-atmosphere transfer scheme (BATS) version 1e as coupled to the NCAR Community Climate Model, *Tech. Rep. NCAR/TN-387 + STR*, 72 pp., Natl. Cent. for Atmos. Res., Boulder, Colo., 1993.
Fowler, W. B., and J. D. Helvey, Effect of large scale irrigation on climate in the Columbia Basin, *Science*, *184*, 121–127, 1974.
Garratt, J. R., Sensitivity of climate simulations to land-surface and atmospheric boundary-layer treatments—A review, *J. Clim.*, *6*, 419–449, 1993.
Giorgi, F., and G. T. Bates, The climatological skill of a regional model over complex terrain, *Mon. Weather Rev.*, *117*, 2325–2347, 1989.
Greenland, D., R. Ingersoll, M. Losleben, and T. R. Seastedt, A decrease in temperatures at high elevations in the Colorado Front Range USA, *Oreg. Geogr.*, *11*, 1–3, 1995.
Gutman, M. P., S. Gonzalez Baker, and S. Pullum, Ethnicity and land use in a changing environment: The Great Plains in the twentieth century, paper presented at Annual Meeting, Popul. Assoc. of Am., Washington, D.C., March 26–29, 1997.
Hansen, J., and S. Lebedeff, Global trends of measured surface air temperature, *J. Geophys. Res.*, *92*, 13345–13372, 1987.
Harrington, J. Y., The effects of radiative and microphysical processes on simulated warm and transition season Arctic stratus, Ph.D. dissertation, 289 pp., Colo. State Univ., Dep. of Atmos. Sci., Fort Collins, 1997.
Henderson-Sellers, A., K. McGuffie, and C. Gross, Sensitivity of a global climate model simulations to increased stomatal resistance and CO2 increases, *J. Clim.*, *8*, 1738–1756, 1995.
Karl, T. R., C. N. Williams Jr., P. J. Young, and W. M. Wendland, A model to estimate the time of observation bias associated with monthly mean maximum, minimum, and mean temperatures for the United States, *J. Clim. Appl. Meteorol.*, *25*, 145–160, 1986.
Küchler, A. W., Potential natural vegetation of the conterminous United States, *Spec. Publ. 36*, Am. Geophys. Soc., New York, 1964.
Lee, T. J., The impact of vegetation on the atmospheric boundary layer and convective storms, *Atmos. Sci. Pap. 509*, 137 pp., Colo. State Univ., Fort Collins, 1992.
Louis, J. F., A parametric model of vertical eddy fluxes in the atmosphere, *Boundary Layer Meteorol.*, *17*, 187–202, 1979.
Loveland, T. R., J. W. Merchant, D. O. Ohlen, and J. F. Brown, Development of a land-cover characteristics database for the coterminous U.S., *Photogramm. Eng. Remote Sens.*, *57*, 1453–1463, 1991.
Mahfouf, J.-F., E. Richard, and P. Mascart, The influence of soil and vegetation on the development of mesoscale circulations, *J. Clim. Appl. Meteorol.*, *26*, 1483–1495, 1987.
Mahrer, Y., and R. A. Pielke, A numerical study of the airflow over irregular terrain, *Beitr. Phys Atmos.*, *50*, 98–113, 1977.
Ookouchi, Y., M. Segal, R. C. Kessler, and R. A. Pielke, Evaluation of soil moisture effects on the generation and modification of mesoscale circulations, *Mon Weather Rev.*, *112*, 2281–2291, 1984.
Pielke, R. A., and M. Segal, Mesoscale circulations forced by differential terrain heating, in *Mesoscale Circulations*, edited by P. Ray, pp. 516–548, Am. Meteorol. Soc., Boston, Mass., 1986.
Pielke, R. A., G. Dalu, J. S. Snook, T. J. Lee, and T. G. F. Kittel, Nonlinear influence of mesoscale land use on weather and climate, *J. Clim.*, *4*, 1053–1069, 1991.
Pielke, R. A., et al., A comprehensive meteorological modeling system—RAMS, *Meteorol. Atmos. Phys.*, *49*, 69–91, 1992.
Pielke, R. A., J. H. Rodriguez, J. L. Eastman, R. L. Walko, and R. A. Stocker, Influence of albedo variability in complex terrain on mesoscale systems, *J. Clim.*, *6*, 1798–1806, 1993.
Pielke, R. A., J. Eastman, T. N. Chase, J. Knaff, and T. G. F. Kittel, 1998: 1973–1996 trends in depth-averaged tropospheric temperature, *J. Geophys. Res.*, *103*, 16927–16933, 1998. (Correction, *J. Geophys. Res.*, *103*, 28909–28911, 1998.)
Poulos, G. S., The interaction of katabatic winds and mountain waves, Ph.D. dissertation, 300 pp., Dep. of Atmos. Sci., Colo. State Univ., Fort Collins, 1996.
Rabin, R. M., and D. W. Martin, Satellite observations of shallow cumulus coverage over the central United States: An exploration of land use impact on cloud cover, *J. Geophys. Res.*, *101*, 7149–7155, 1996.
Reynolds, R. W., and T. M. Smith, Improved global sea surface temperature analyses using optimal interpolation, *J. Clim.*, *7*, 929–948, 1994.
Segal, M., R. Avissar, M. C. McCumber, and R. A. Pielke, Evaluation of vegetation effects on the generation and modification of mesoscale circulations, *J. Atmos. Sci.*, *45*, 2268–2292, 1988.
Segal, M., W. E. Schreiber, G. Kallos, J. R. Garratt, A. Rodi, J. Weaver, and R. A. Pielke, The impact of crop areas in northeast Colorado on midsummer mesoscale thermal circulations, *Mon. Weather Rev.*, *117*, 809–825, 1989.
Seth, A., and F. Giorgi, Three-dimensional model study of organized mesoscale circulations induced by vegetation, *J. Geophys. Res.*, *101*, 7371–7391, 1996.
Smagorinsky, J., General circulation experiments with the primitive equations, 1, The basic experiment, *Mon. Weather Rev.*, *91*, 99–164, 1963.
Stohlgren, T. J. T. N. Chase, R. A. Pielke, T. G. F. Kittel, and J. S. Baron, Evidence that local land use practices influence regional climate and vegetation patterns in adjacent natural areas, *Global Change Biol.*, *4*, 495–504, 1998.
Sud, Y. C., J. Shukla, and Y. Mintz, Influence of land surface roughness on atmospheric circulation and precipitation: A sensitivity study with a general circulation model, *J. Appl. Meteorol.*, *27*, 1036–1054, 1988.
Toth, J. J., and R. H. Johnson, Summer surface flow characteristics over northeast Colorado, *Mon. Weather Rev.*, *113*, 1458–1468, 1984.
Tremback, C. J., and R. Kessler, A surface temperature and moisture parameterization for use in mesoscale numerical models, paper presented 7th Conference on Numerical Weather Prediction, Am. Meteorol. Soc., Montreal, Canada, June 17–20, 1985.
Vidale, P. L., Contributions of land surface forced mesoscale circulations to the total heat, moisture, and momentum budgets over BOREAS, Ph.D. dissertation, Dep. of Atmos. Sci., Colo. State Univ., Fort Collins, 1998.
Vinnikov, K. Y., P. Y. Groisman, and K. M. Lugina, Global and hemispheric temperature anomalies from instrumental surface air temperature records, in *Trends '93: A Compendium of Data on Global Change ORNL/CDIAD-65*, pp. 615–627, Carbon Dioxide Information Anal. Cent., Oakridge Natl. Lab., Oakridge, Tenn., 1994.
Walko, R. L., W. R. Cotton, M. P. Meyers, and J. Y. Harrington, New RAMS cloud microphysics parameterization, I, The single moment scheme, *Atmos. Res.*, *38*, 29–62, 1995.
Wenger, R., Zur theorie der Berg-undtalwinde, *Meteorol. Z.*, *40*, 193–204, 1923.
Williams, M. W., M. Losleben, N. Caine, and D. Greenland, Changes in climate and hydrochemical responses in a high-elevation catchment in the Rocky Mountains, USA, *Limnol. Oceanogr.*, *41*, 939–946, 1996.
Wolyn, P. G., and T. B. McKee, The mountain-plains circulation east of a 2-km-high north-south barrier, *Mon. Weather Rev.*, *122*, 1490–1508, 1994.
Zhang, D. L., and R. A. Anthes, A high resolution model of the planetary boundary layer—sensitivity tests and comparisons with SESAME-79 data, *J. Appl. Meteorol.*, *21*, 1594–1609, 1982.
Zhang, H., A. Henderson-Sellers, and K. McGuffie, Impacts of tropical deforestation, I, Process analysis of local climate change, *J. Clim.*, *9*, 1497–1517, 1996.

J. S. Baron and T. J. Stohlgren, Midcontinent Ecological Science Center, Biological Resources Division, U.S. Geological Survey, 4512 McMurray Avenue, Fort Collins, CO 80525. (jill@nrel.colostate.edu)
T. N. Chase and R. A. Pielke Sr., Department of Atmospheric Science, Colorado State University, Fort Collins, CO 80523. (chase@deathstar.atmos.colostate.edu; dallas@hercules.atmos.colostate.edu)
T. G. F. Kittel, Climate and Global Dynamics Division, National Center for Atmospheric Research, Box 3000, Boulder, CO 80307-3000. (kittel@ucar.edu)

(Received July 12, 1998; revised January 26, 1999;
accepted February 4, 1999.)